Cerebellum (2015) 14:175–196
DOI 10.1007/s12311-014-0610-3

CONSENSUS PAPER

Consensus Paper: Radiological Biomarkers of Cerebellar Diseases

Leonardo Baldarçara · Stuart Currie · M. Hadjivassiliou · Nigel Hoggard · Allison Jack · Andrea P. Jackowski · Mario Mascalchi · Cecilia Parazzini · Kathrin Reetz · Andrea Righini · Jörg B. Schulz · Alessandra Vella · Sara Jane Webb · Christophe Habas

Published online: 11 November 2014

Abstract Hereditary and sporadic cerebellar ataxias represent a vast and still growing group of diseases whose diagnosis and differentiation cannot only rely on clinical evaluation. Brain imaging including magnetic resonance (MR) and nuclear medicine techniques allows for characterization of structural and functional abnormalities underlying symptomatic ataxias. These methods thus constitute a potential source of radiological biomarkers, which could be used to identify these diseases and differentiate subgroups of them, and to assess their severity and their evolution. Such biomarkers mainly comprise qualitative and quantitative data obtained from MR including proton spectroscopy, diffusion imaging, tractography, voxel-based morphometry, functional imaging during task execution or in a resting state, and from SPETC and PET with several radiotracers. In the current article, we aim to illustrate briefly some applications of these neuroimaging tools to evaluation of cerebellar disorders such as inherited cerebellar ataxia, fetal developmental malformations, and immune-mediated cerebellar diseases and of neurodegenerative or early-developing diseases, such as dementia and autism in which cerebellar involvement is an emerging feature. Although these radiological biomarkers appear promising and helpful to better understand ataxia-related anatomical and physiological impairments, to date, very few of them have turned out to be specific

L. Baldarçara
Federal University of Tocantins, Tocantins, Brazil

L. Baldarçara · A. P. Jackowski
Federal University of São Paulo, São Paulo, Brazil

S. Currie · N. Hoggard
Academic Unit of Radiology, University of Sheffield, Royal Hallamshire Hospital, Sheffield, UK

M. Hadjivassiliou
Academic Department of Neurosciences, Royal Hallamshire Hospital, Sheffield, UK

A. Jack
Child Study Center, Yale University, New Haven, CT, USA

M. Mascalchi
"Mario Serio" Department of Experimental and Clinical Biomedical Sciences, University of Florence, Florence, Italy

M. Mascalchi
Quantitative and Functional Neuroradiology Research Program at the Meyer Children and Careggi Hospital of Florence, Florence, Italy

C. Parazzini · A. Righini
Pediatric Radiology and Neuroradiology Department, Children's Hospital V. Buzzi, Milan, Italy

K. Reetz · J. B. Schulz
Department of Neurology, RWTH Aachen University Hospital, Aachen, Germany

K. Reetz
Institute of Neuroscience and Medicine (INM-4), Research Centre Jülich GmbH, Jülich, Germany

K. Reetz · J. B. Schulz
Jülich Aachen Research Alliance (JARA)—Translational Brain Medicine, Aachen, Germany

A. Vella
Nuclear Medicine Unit, Policlinico "Le Scotte", University Hospital of Siena, Italy, Siena, Italy

S. J. Webb
Center for Child Health, Behavior and Development, Seattle Children's Research Institute, Department of Psychiatry & Behavioral Sciences, University of Washington, Seattle, WA, USA

C. Habas (✉)
Service de NeuroImagerie, CHNO des Quinze-Vingts, Paris, France
e-mail: chabas@quinze-vingts.fr

for a given ataxia with atrophy of the cerebellar system being the main and the most usual alteration being observed. Consequently, much remains to be done to establish sensitivity, specificity, and reproducibility of available MR and nuclear medicine features as diagnostic, progression and surrogate biomarkers in clinical routine.

Keywords Cerebellum · Ataxia · Autism · Dementia · Radiological biomarker · Immunity · Fetal malformation · MRI · fMRI · Spectroscopy · Diffusion · SPECT · PET · Ultrasound

Introduction

Neuroimaging, including magnetic resonance imaging and single-photon emission computed tomography (SPECT)/positron emission tomography (PET), provides several and potential valuable biomarkers for diagnosis, prognosis, and follow-up of the course of cerebellar diseases. Conventional MRI sequences (T1, T2, T2*, FLAIR, STIR, diffusion, magnetic susceptibility, angiography) supply macroscopic clues for anatomical localization and diagnosis of a wide range of cerebellar alteration (for example: malformations, tumor, stroke, infection, and inflammation) including especially recessively and X-linked inherited ataxias. However, these MRI sequences can fail to detect subtle histological or biochemical alteration, to differentiate properly subtypes of a given disease, and to establish robust anatomoclinical correlations. This is particularly the case for cerebellar ataxias and some neurodegenerative and neurodevelopmental diseases in which also the cerebellum appears to be affected [1, 2]. SPECT/PET using radiotracers of perfusion and glucose metabolism primarily contribute to search for brain hypoperfusion or hypometabolism [1]. Unconventional MRI techniques and utilization of more specific SPECT or PET radiotracers may widen the scope of neuroimaging in ataxia diseases and partly overcome some of the above limitations. First, unconventional MRI allows a thorough qualitative and quantitative characterization not only of gross anatomical alterations of the cerebellar system using, for instance, volume-based morphometry (VBM), but also of cerebellar microstructural tissue organization with measurement of the apparent diffusion coefficient (ADC) in diffusion-weighted imaging (DWI) and with tractography performed on diffusion tensor imaging (DTI), which can compute anatomical bundles composing the white matter. Second, mono- and multi-voxel proton spectroscopy can identify biochemical alterations of the white and gray matter measuring different molecules such as *N*-acetyl-aspartate (neuronal biomarker), choline (membrane biomarker) myo-inositol (gliosis biomarker) or lactate (anaerobic metabolism biomarker). Third, several radiotracers can be utilized in nuclear medicine to detect or track specific regional dysfunctions, as that of the nigrostriatal pathway, and to clarify their underlying physiopathological mechanisms. Fourth, functional MR imaging during task execution or in a resting state may estimate disease-related functional alterations and reorganization (neuroplasticity) of the whole cerebellar system with potential correlation with clinical deficits and recovery. Fifth, pre- and postnatal ultrasound and MRI enable to follow and to detect early fetal developmental anomalies.

In the current article, we aim to illustrate briefly some applications of these neuroimaging tools, especially unconventional MRI techniques and SPECT/PET, in the evaluation of cerebellar disorders such as cerebellar ataxia (see Sections 1 and 2), fetal developmental malformations (see Section 3), autosomal dominant spinocerebellar ataxia (see Section 4), immune-mediated cerebellitis (see Section 5) and to characterization of cerebellar involvement in neurodegenerative diseases as dementia (see Section 6) and autism (see Section 7), recessive and X-linked hereditary ataxias (see Section 8), metabolic ataxias in children (see Section 9), and multiple systems atrophy and sporadic adult-onset ataxia of unknown etiology (see Section 10). Apart from macroscopic cerebellar disorganization due to developmental malformations, the most frequent alteration observed in MRI consists of regional atrophy mainly affecting more or less specific cerebellar lobes/lobules, pons (spinocerebellar ataxia (SCA), dementia, autism) and striatum (SCA1 and SCA3). Other alterations, sometimes in association with regional atrophy include: (1) microstructural abnormalities such as increased ADC in DWI and decreased fractional anisotropy (FA) in DTI (SCAs and Friedreich's ataxia), (2) decreased or increased cerebellar perfusion or metabolism (dementia, paraneoplastic syndrome, post-infection cerebellitis, multi system atrophy—cerebellar type, pure cerebellar ataxia) in SPECT or PET, and (3) proton MR spectroscopy alterations such as reduction of *N*-acetyl-aspartate (NAA) in gluten ataxia and SCAs. Functional connectivity of motor and cognitive cerebello-cortical networks proved to be altered in SCA17. Interestingly, presymptomatic carriers of several SCA subtypes exhibited nigrostriatal dysfunction and cerebellar hypometabolism. Nevertheless, no biomarker turns out to be specific of a given pathology. Furthermore, some anatomoclinical correlation exist, for example, between specific atrophy of the anterior or posterior lobes and motor and neuropsychological atrophy (SCA, dementia) respectively, between increased ADC and clinical dysfunction (SCA1 and SCA2) or mean diffusivity (MD) increase and fractional anisotropy (FA) decrease and severity of ataxia [multiple system atrophy (MSA), Friedreich ataxia]. Concerning dementia or autism, biomarkers could be used not for diagnosis per se but to assess disease evolution and cerebellar involvement in neuropsychological-associated deficits.

While currently available radiomarkers undoubtedly help to better identify in vivo histological, anatomical,

biochemical, and pathophysiological changes of some cerebellar diseases, they still lack specificity to fully and differentially characterize them. Further studies are thus required to evaluate the specific profile of combined radiomarkers to univocally identify a given cerebellar disease, to draw precise anatomoclinical correlations, to anticipate disease evolution and to test response to treatments. It could be also postulated that multivariate statistical analyses (principal component analysis, discriminant analysis, machine learning approaches) using a set of such biomarkers would be more powerful for diagnosis and prognosis than a single biomarker alone. For example, principal component analysis successfully discriminates two different patterns of cerebellar degeneration observed in SCA2 and SCA 6 [3]. This notwithstanding, such useful and promising "unconventional" biomarkers should from now on be incorporated to routine neuroimaging investigation of cerebellar diseases. The following can be recommended to apply at least and in complement with conventional MRI: (1) volumetric T1-weighted sequences for VBM to search for atrophy of the cerebellum, brainstem and striatum; (2) measurement of ADC in DWI and/or FA in DTI to appreciate associated tissue disorganization and cellular loss, (3) ^{1}H spectroscopy to detect abnormal biochemical profile, (4) DTI and functional MRI to estimate structural and functional network impairment, and (5) SPECT/PET to seek for striatal and extra-striatal changes in MSA. More specifically, MRI patterns of regional cerebellar and brainstem atrophy, in some instances in combination with a characteristic distribution of signal or microstructural changes, are helpful diagnosis and evolution biomarkers of spinocerebellar, recessive (such as Joubert syndrome, Friedreich's ataxia, ataxia telangiectasia, autosomal recessive spastic ataxia of Charlevoix and Saguenay, cerebrotendineous xanthomatosis, and X- fragile tremor ataxia syndrome), and metabolic ataxias. Cerebellar atrophy combined with high lactate peak within the cerebellum seems strongly in favor of mitochondropathy-related cerebellar ataxia. Except lactate, abnormal peaks such as elevated *N*-acetyl-aspartate, galacticol or phenylalanine, may suggest specific metabolic ataxia. Moreover, decreased NAA/choline ratio below 5.0 might predict progression of X-linked adrenoleucodystrophy (evolution biomarker). Concerning nuclear medicine, three techniques can be applied for specific diagnoses: brain perfusion SPECT to detect early cerebellar blood flow abnormalities in cerebellitis, whole-body fluorodeoxy-glucose PET (FDG-PET) in case of suspected paraneoplastic cerebellar degeneration syndrome and clinically occult primary malignancy, and brain FDG-PET and dopamine transport imaging in case of MSA. Although some cerebellar abnormalities may exist, MRI does not provide important data for diagnosis of immune ataxia, dementia, and autism. Some cerebellar abnormalities could be linked to severity of the disease and predict impaired behavioral outcome, but further studies are required to validate these points.

Lastly, fetal MRI can complement ultrasound data to study white matter myelination, small necrotic-hemorrhagic lesion, and potential extracerebellar-associated lesions.

Section 1: Radiological Biomarkers of Cerebellar Ataxia

Imaging modalities including computed tomography (CT), magnetic resonance imaging (MRI), single-proton emission computed tomography (SPECT) and positron emission tomography (PET) have been widely utilized in the investigation of patients with ataxia [1, 2]. CT is typically limited to the evaluation of hemorrhage or mass lesion within the posterior fossa and it has virtually no role in the temporal assessment of patients with chronic ataxia. MRI is the imaging technique most frequently employed in the assessment of patients with ataxia. The high spatial and contrast resolution, in combination with multiplanar reformatting allows in vivo evaluation of regional atrophy, which may reveal a distribution pattern suggestive of a particular condition. Three fundamental patterns of atrophy that correspond with gross neuropathological findings are repeatedly described in the literature and include olivopontocerebellar atrophy, cortical cerebellar atrophy, and spinal atrophy. Such descriptive patterns have been substantially applied to the etiological classification of chronic ataxias and can help to narrow a broad differential diagnosis. T2 signal changes in characteristic locations can provide further indicators of certain conditions such as multiple system atrophy, Wernicke encephalopathy, and superficial siderosis [2].

In the clinical setting, assessment of volume loss in a single patient remains largely subjective but with experience a reliable grading system may be achieved and can be applied sequentially to provide chronological appraisal. Midsagittal T1-weighted images enable the inspection of the brainstem and vermis while parasagittal, axial or coronal planes allow scrutiny of the cerebellar hemispheres and peduncles [4] Subjective assessment is limited by interobserver disagreement and on its dependence on observer experience. It may also lack sensitivity for the detection of changes early in the disease or at a subclinical phase. More quantitative measurements of brain atrophy may be provided with MRI-based volumetry whereby volumes of individual brain structures are determined via manual or automated segmentation [5] or by way of voxel-based morphometry (VBM), an operator-independent tool used to detect regionally specific differences in brain tissue composition on a voxel by voxel basis [6]. VBM is dependent on tissue segmentation, which ultimately requires the correct identification of gray and white matter and CSF partitions. In areas where gray/white matter differentiation is poor, voxels may be incorrectly classified. This is especially true in the posterior fossa and acts to reduce sensitivity [3]. Quantitative volumetric techniques remain largely confined to group analysis and they have been primarily

employed as surrogate markers of disease progression in clinical research. A similar synopsis may be applied to non-conventional MR techniques such as diffusion, spectroscopy, magnetization transfer, and functional MRI. Biomarkers obtained through these sequences that offer quantitative assessment of microstructural integrity including apparent diffusion coefficient (ADC), fractional anisotropy (FA), and magnetization transfer ratio (MTR) have been largely evaluated in studies that have attempted to differentiate groups of patients with different diagnoses of ataxia. While the literature is generally supportive of a role for these MRI techniques for cohort analysis, their value in a single patient remains unclear. The use of non-conventional MRI techniques as reproducible biomarkers of ataxia at the individual level ultimately requires the use of validated and robust techniques, which, when devoid of consensus multicenter data (as is currently the case), can be measured at the local institutional level against normal data obtained using the same imaging protocol. In these conditions, single-voxel ^{1}H MR spectroscopy has been used successfully in the surveillance of patients with paraneoplastic cerebellar degeneration with temporal changes in *N*-acetyl aspartate, a marker of neuronal health and integrity, reportedly mirroring tumor progression/regression [7]. A role for MR spectroscopy in monitoring the temporal changes in cerebellar neurometabolites in relation to dietary treatment has also been reported in patients with gluten ataxia [8]. Further evaluation of metabolites obtained at short echo time (such as glutamate) may provide indicators of cerebellar disease but currently this remains unclear.

Section 2: Biomarkers of Cerebellar Ataxia in Nuclear Medicine

Three main types of radiotracers for SPECT or PET have been utilized with different aims to investigate patients suffering from acute or chronic ataxia [1].

Evaluation of regional blood flow with single-photon emission tracers, including [^{99m}Tc]-HM-PAO, [^{123}I]-IMP, and [^{99m}Tc]-ECD, has found two indications for diagnostic purposes in the single patient, namely early diagnosis of cerebellitis, that is characterized by increased or decreased cerebellar flow, and differential diagnosis between idiopathic late-onset cerebellar ataxia (pure) (ILOCA) and multi system atrophy-cerebellar type (MSA-C) with demonstration of more pronounced pontine hypoperfusion in the latter [1]. Regional perfusion was correlated with clinical features in spinocerebellar ataxia type 3(SCA3) [9], SCA6 and ataxia telangectasia [1]. More importantly, SPECT perfusion data were recently utilized as surrogate biomarkers of the efficacy of thyrotropin releasing hormone or immunoglobulin therapy in pilot studies of degenerative and autoimmune ataxias and documented increased cerebellar blood flow in line with clinical improvement in patients with ILOCA, SCA6, or autoantibody-positive cerebellar ataxia, but not in those with MSA [10–12].

Mapping brain metabolism with the positron emission tracer [^{18}F]-FDG and head PET can support the diagnosis of MSA by revealing a distributed and progressive hypometabolism of the cerebellum, pons, basal ganglia, and frontal and parietal cerebral cortex [1, 13]. However, the more important clinical application of [^{18}F]-FDG in ataxias is the whole-body PET examination in search of occult primary malignancy in patients with suspected paraneoplastic cerebellar degeneration [14]. Head [^{18}F]-FDG-PET has also been extensively used for physiopathological characterization of chronic inherited or sporadic ataxias [1, 15]. In particular, it documented early hypometabolic areas in presymptomatic carriers of SCA2, SCA3, and SCA17 mutation [16–18] and showed variable correlation with severity of neurological deficit in cross-sectional studies [1]. In one recent study, three patients with cerebellar ataxia associated with antibodies against glutamic acid decarboxylase were examined with head [^{18}F]-FDG before and after intravenous immunoglobulin and no further decline of metabolism in the cerebellum was observed in the two patients with amelioration of cerebellar ataxia following immunoglobulin therapy [19].

Several single-photon or positron emission tracers are available to explore nigrostriatal function with SPECT or PET. The SPECT tracers include ligands of the dopamine active transporter (DaT) as [^{123}I]FP-CIT, [^{123}I]-2b-CIT, and [^{99m}Tc]-TRODAT-1 and of the postsynaptic D2 receptors as [^{123}I]-IBZM. SPECT with DaT tracers, comprehensively called DaT-Imaging, can support the diagnosis of MSA by demonstrating decreased striatal uptake, which is typically combined with decreased striatal D2 receptors [1]. They were also extensively utilized for physiopathological characterization of other chronic inherited or sporadic ataxias [1]. PET tracers of nigrostriatal function including [^{18}F]-FDopa and ligands of striatal dopamine transporter as [^{11}C]d-MP and of D2 receptors as [^{11}C]-raclopride have been used for the same purposes with similar results to those obtained with SPECT tracers [1]. Notably, nigrostriatal dysfunction was observed in presymptomatic carriers of the SCA2, SCA3, SCA6, and SCA17 genes [1, 18, 20, 21].

A last group of positron emission tracers including ligands of GABA/benzodiazepine receptors as [^{11}C]-FMZ and markers of the acetylcholinesterase activity as [^{11}C]-PMP was used for physiopathological characterization of chronic inherited or sporadic ataxias [1, 19].

Overall, in patients with ataxias, despite the relatively large number of nuclear medicine studies and the valuable contribution that SPECT and PET can provide for diagnosis in the single patient and to understand the physiopathology of ataxia disorders, there is relative paucity of data about the capability of SPECT and PET to track progression of disease or to serve

as surrogate markers for new treatments [1, 10–12, 19]. Noteworthy and of potential major impact for these crucial applications is incorporation in a recent study of PET with a striatal D2 receptor marker, namely [^{11}C]-raclopride, in the assessment of an animal model of SCA17 [22].

Section 3: Radiological Biomarkers of Fetal Cerebellar Developmental Alterations

State of the art ultrasound (US), performed by expert neurosonographers and by using 3D-reformatted technique, is able to detect the majority of fetal cerebellar anomalies [23], such as hypoplasia, rhombencephalosynapsis, cystic malformations as Dandy-Walker, and large necrotic-hemorrhagic lesions. However, in some abnormal conditions, fetal magnetic resonance (MR) imaging may add additional and valuable information [24].

When fetal MR scanning begins to be performed in clinical setting (usually around the 18th–20th week of gestation), the general final shape of the cerebellum is already recognizable on multiplanar ultrafast T2-weighted (3–5 mm thick) sections: the vermis in its final position, almost adhering to the fourth ventricle floor on midsagittal section; the primary fissure visible in most cases; middle cerebellar peduncles clearly visible, especially on axial sections. It is important to assess the relationship between cerebellar vermis and the pontine bulging, the level of tentorium occipital insertion (normally at nuchal muscles insertion level), and the dimension of the cisterna magna [25]. Linear biometry of the vermis and cerebellar hemispheres is usually assessed [26]. Later during the pregnancy, the volume of cerebellum accelerates its growth [27]; close to the 30th week of gestation, additional vermian fissures are often recognizable on midsagittal image, and the hypointense signal of myelination is noticeable in the pontine tegmentum.

Clastic Lesions MR imaging may highlight smaller necrotic-hemorrhagic hemispheric lesions better than US. They are mostly of unknown etiology, often unilateral, located in the caudal part of cerebellar hemispheres, involving or not the vermis; such lesions usually appear as T2-hypointense foci, with some superficial filaments or micro-cysts (probably due to arachnoid reaction), and sometimes with hyperintense T1 spots. They usually tend to evolve toward cerebellar hemiatrophy [28], with areas of irregularly invaginated and oriented folia. When hemosiderin deposits are no longer visible in postnatal MR imaging, it may be difficult to differentiate such lesions from those of genetic etiology.

Cerebellum–Pontine Hypoplasia 3D-US is usually sufficient to highlight significant cerebellum and pons volume reduction in these non clastic anomalies; however, MR imaging may help to exclude associated intracranial pathologies and to prove that the entire cerebellum is usually decreased in size.

Complex Malformations The diagnosis of some complex malformations of cerebellum and brainstem, such as molar tooth group, incomplete non classical rhombencephalosynapsis, brainstem kinking in muscle-eye brain diseases, pontine-tegmental cap or still unclassified and emerging ones, such as bilateral foliation orientation derangement, may benefit from MR imaging, especially before the 24th week of gestation; the features of such malformations are usually similar to the ones of postnatal MR imaging, but, because of the limited spatial resolution, a definite diagnosis may still be very difficult in utero; in these cases, the use of higher-resolution (2 mm thick) true-FISP or BALANCE sections may be advised.

Upward Rotation of Cerebellar Vermis This is one of the still most challenging conditions in prenatal counselling, albeit one the most frequent. Not totally definable and still unclear vermian entities, such as "caudal hypoplasia", "incomplete rotation", "Dandy-Walker variant", challenge the reproducibility of scientific reports on this regard and the possibility of a reliable prognosis. MR imaging may complement US in order to better deal with such conditions, especially by excluding the possibility of other intracranial anomalies [29]. When vermian upward rotation (cerebellar-pontine angle above 8–10°) is really isolated (normal karyotype, no other intracranial or body anomalies at prenatal imaging, normal latero-lateral cerebellar diameter, and normal brainstem appearance), the probability of a good prognosis is higher than 80 %, with many cases undergoing even angle normalization [30]; however, fetal MR imaging is currently still unable to identify that minority of cases, which will experience significant behavioural and neurological anomalies.

In summary, main prenatal MR imaging markers, which help to differentiate between clastic- and genetic-based cerebellar anomalies are: (1) in favour of a clastic etiology: presence of unilateral anomaly with focal hemispheric surface distortion (i.e., paravermian unilateral cleft), presence of hemosiderine deposits, associated clastic signs in supratentorial compartment (i.e., cerebral hemorrhages or parenchymal edema, T1-weighted hyperintense foci of cortical necrosis, lateral ventricles septa and sinechiae), cysts within the tip of temporal lobes (as in CMV infection), venous sinuses engorgement, (2) in favor of a genetic etiology: presence of very symmetric bilateral dysmorphism (i.e., folia malorientation), vermian hypoplasia and upward rotation with clearly enlarged posterior fossa, associated brainstem anomalies (i.e., midline cleft, megatectum, pontine cap), associated skull anomalies (i.e., occipital encephalocele), associated supratentorial anomalies (i.e., short corpus callosum, hippocampal malrotation, reduced opercularization, band

heterotopias), associated head-neck anomalies (i.e., palatine schisis, optic nerve head coloboma).

Section 4: Structural and Functional Neuroimaging in Autosomal Dominant Spinocerebellar Ataxias

Autosomal dominant spinocerebellar ataxias (SCAs) are a heterogeneous group of progressive neurodegenerative disorders, caused by diverse genetic mutation types and complex pathogenesis, and clinically mainly characterized by cerebellar ataxia, including unsteady gait, clumsiness, and dysarthria. The cerebellar syndrome is often associated with other neurological signs such as pyramidal or extrapyramidal symptoms, ophthalmoplegia, and cognitive impairment. Onset is generally during the third or fourth decade of life, but can also occur in childhood or elderly. Atrophy of the cerebellum and brainstem are most often the prominent imaging features, but other structures can be also affected, leading to a wide range of phenotypes. Longitudinal studies indicate further that there might also be a disease-related, genotype-specific staging progression of neurodegeneration patterns. Correlations between phenotype and genotype in the polyglutamine expansion have shown that differences in repeat size may contribute to age at onset, disease progression, severity, and clinically different phenotypes between patients. Functional imaging studies have further enhanced a better understanding of pathological findings and their association to clinical features in these disorders. As most neuroimaging data are available for the more common subtypes SCA1, SCA2, SCA3, SCA6, SCA7, and SCA17, they are described in more detail in the following. Major magnetic resonance imaging (MRI) characteristics are schematically presented in Fig. 1. An overview for all SCAs is given in Table 1.

Structural neuroimaging in SCA1 revealed atrophy predominantly in the brainstem, cerebellum, and basal ganglia [31, 32]. Even in preclinical SCA1 mutation carriers compared to non-carriers gray matter loss in the medulla oblongata and pons was detectable [33]. Compared to other SCAs, the typical olivo-ponto-cerebellar atrophy in SCA1 was described as similar but not as severe as in SCA2 [31, 34] and more prominent than in SCA3 with respect to the cerebellar hemispheres [32]. A longitudinal MRI study, combining quantitative volumetry and voxel-based morphometry (VBM), revealed that pontine volume was the most sensitive measure of disease in SCA1, which was superior to the most sensitive clinical measure, the Scale for the Assessment and Rating of Ataxia [35]. There was further a mild correlation between CAG repeat length and volume loss in the bilateral cerebellum

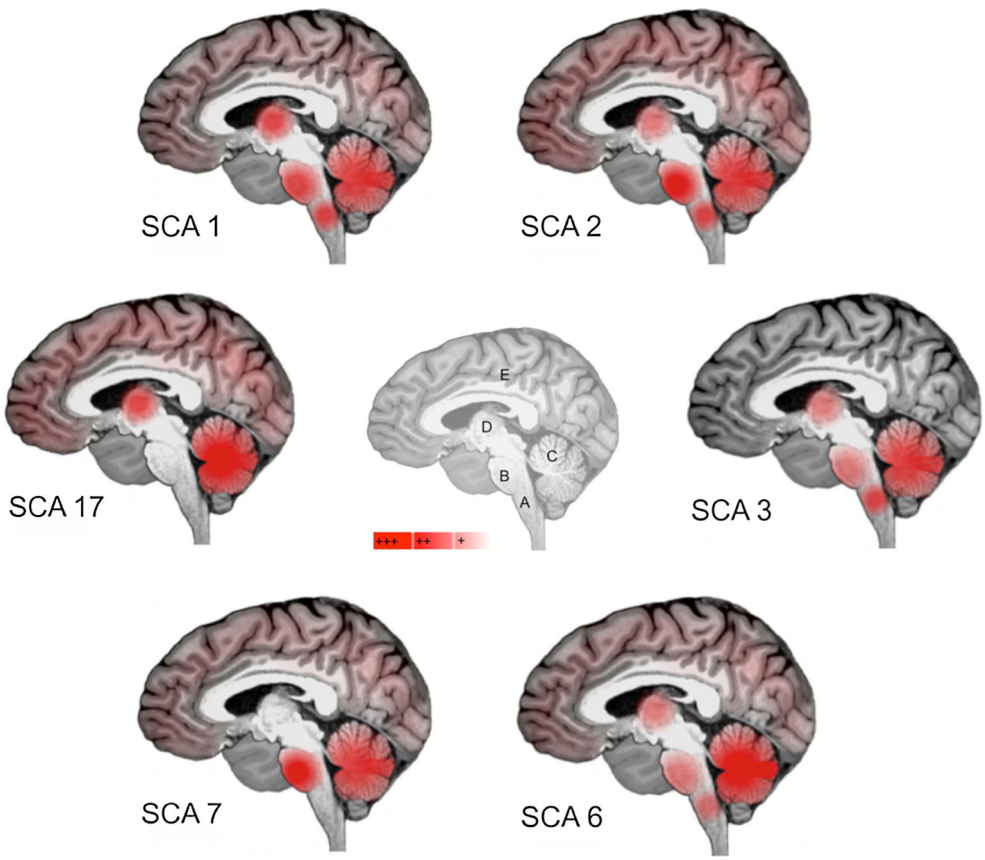

Fig. 1 Schematic representation of the main sites of atrophy (*in red*) observed in SCA 1, 2, 3, 6, 7 and 17 (*A* medulla oblongata; *B* pons, *C* cerebellum, *D* basal ganglia, *E* cerebral cortex) on sagittal view of the brain

Table 1 The spinocerebellar ataxias

SCA	Gene/locus	Mutation type	Key symptoms in addition to cerebellar ataxia	MRI characteristics (atrophy)					
				Brainstem	Pons	Cerebellar hemispheres	Vermis	Basal ganglia	Cortical areas
1	ATXN1/6p22.3	CAG repeat	Dysphagia	++	++	++	++	++	+
2	ATXN2/12q24.12	CAG repeat	Oculomotor symptoms	++	+++	++	++	(+)	++
3	ATXN3/14q32.12	CAG repeat	Dystonia, parkinsonism, neuropathy	++	+	++	++	+	
4	/16q21.1	Unknown	Sensory neuropathy			+	+		
5	SPTBN2/11q13.2	Missense, n-frame deletion	Nystagmus	−	−	++	++	−	−
6	CACNA1A/19p13.2	CAG repeat		+	+	+++	+++	+	(+)
7	ATNX7/3p14.1	CAG repeat	Visual loss		+++	++	++		+
8	ATXN8OS/13q21	CTG repeat	Sensory neuropathy, spasticity	−	−	++	++		−
9	Unknown	Unknown	Ophthalmoplegia, pyramidal and extrapyramidal signs						
10	ATXN10/22q13.31	ATTCT	Epilepsy	−		++	++		
11	TTBK-2/15q15.2	Frameshift	Nystagmus			+	+		
12	PPP2R2B/5q32	CAG repeat	Tremor	−	−	+	+	−	+
13	KCNC3/19q13.33	Point mutation	Mental retardation	+	+		+		
14	PRKCG/19q13.42	Missense, deletion	Myoclonus		(+)	++	++	−	−
15/16	ITPR1/3p26.1	Missense, frameshift	Tremor	−	−	+	++		
17	TBP/6q27	CAG repeat	Dementia, psychiatric disorders			+++	++	++	++
18	/7q22-32	Unknown	Sensory neuropathy, muscle atrophy			+	+		(+)
19/22	KCND3/1p21-q21	Unknown	Mental retardation			+	+		(+)
20[a]	/11q12	260 kb duplication	Dysphonia, myoclonus			++	++		
21	/7p21.3-p15.1	Unknown	Mental retardation			+	+		
23	PDYN/20p13	Missense mutation	Sensory neuropathy, pyramidal signs			+	+		
24	/1p36	Unknown	Pyramidal signs, axonal polyneuropathy						
25	/2p21-13	Unknown	Sensory neuropathy, gastrointestinal features	−	−	++	++		
26	/19p13.3	Unknown		−	−	++	++		
27	FGF14/13q33.1	Point mutation	Dyskinesia, metal retardation	−	−	++	++	−	−
28	AFG3L2/18p11.21	Missense mutation	Oculomotor symptoms	−	−	++	++		−
29	ITPR1/3p26	Missense mutation	Cognitive impairment						
30	/4q34.3-q35.1	Unknown							
31	TK2, BEAN/ 16q21	TGGAA repeat	Muscular hypotonia, auditory dysfunction						
32	/7q32-q33	Unknown							
34	/16p12.3-q16.2	Unknown	Cutaneous plaques						
35	TGM6/20p13	Missense mutation	Oculomotor symptoms						

Table 1 (continued)

SCA	Gene/locus	Mutation type	Key symptoms in addition to cerebellar ataxia	MRI characteristics (atrophy)					
				Brainstem	Pons	Cerebellar hemispheres	Vermis	Basal ganglia	Cortical areas
36	NOP56/20q13	Repeat expansion	Mus spasticity, fasciculations, atrophy of tongue and skeletal muscles						

AFG3L2 ATPase family gene 3 like 2, *ATXN* ataxin, *BEAN* brain expressed associated with NEDD-4, *CACNA1A* calcium channel voltage-dependent P/Q type alpha 1A subunit, *FGF14* fibroblast growth factor 14, *ITPR1* inositol triphosphate receptor type 1, *KCNC3* potassium voltage-gated channel Shaw-related subfamily member 3, *KCND3* potassium voltage-gated channel subfamily D member 3, *NOP56* ribonucleoprotein, *PDYN* prodynorphin, *PPP2R2B* serine/threonine-protein phosphotase 2A, *PRKCG* protein kinase C gamma type, *SPTBN2* beta-III-spectrin, *TBP* TATA-box binding protein, *TK2* thymidine kinase 2, *TGM6* transglutaminase 6, *TTBK2* tau tubulin kinase 2, − no atrophy, *(+)* mild/inconsistently reported, + mild atrophy, ++ moderate atrophy, +++ severe atrophy, *blank* not reported/unknown

[a] Calcifications of dentate nucleus

and the pons in SCA1. The ponto-cerebellar brunt in SCA1 is further supported by alterations in white matter, as assessed with VBM and diffusion tensor imaging (DTI) including mean diffusivity (MD) and Tract-based spatial statistics (TBSS) [35, 36]. Structural and functional connectivity analyses using functional MRI and DTI revealed a loss of intrinsic organization of cerebellar networks, which correlated with disease severity and duration in this disconnection syndrome [37].

MRI in SCA2 revealed marked atrophy of the cerebellum, pons, medulla oblongata, and spinal cord, and also showed an involvement of the parietal cortex and thalamus [38, 39]. In preclinical stages, volumetric analyses showed reduced normalized brainstem volumes of SCA2 mutation carriers compared with non-carriers [33]. Using clinical and neuropsychological assessments impaired coordination was linked to atrophy in the anterior cerebellum and executive impairment to atrophy in the posterior cerebellum [38], and ponto-cerebellar volume loss was associated with decreased functional staging scores.

Patterns of ponto-cerebellar atrophy in the worldwide most common SCA3 have been reported in several neuroimaging studies, which is similar but less severe to SCA1, SCA2 (regarding pons), or SCA6 (regarding cerebellum) [31, 32, 34]. MRI revealed further atrophy in the superior cerebellar peduncles, frontal and temporal lobes, as well as diminished transverse diameter of the pallidum. The involvement of the basal ganglia in SCA3 has also been described in previous volumetric measurements [31]. Quantitative three-dimensional volumetry and VBM demonstrated severe atrophy in total brainstem, pons, medulla, total cerebellum, cerebellar hemispheres and cerebellar vermis, putamen and caudate nucleus in SCA3 [32]. The role of putaminal volume loss in SCA3 was underlined further by a 2-year follow-up MRI study revealing most pronounced changes in the putamen [33].

Neuroimaging studies in SCA6 reported moderate to severe atrophy of the vermis, mild atrophy of the cerebellar hemispheres, but no atrophy of the middle cerebellar peduncles, pons or other structures of the posterior fossa [39, 40]. Notably, mild, diffuse atrophy of cortical areas has been described in some SCA6 patients [35]. A cross-sectional volumetric and VBM study showed atrophy in SCA6 predominantly in the cerebellum but also in total brainstem and pons [32], and longitudinally, the most sensitive area to volume loss was the caudate [35]. Longitudinal VBM showed the greatest gray matter loss in the cerebellum, thalamus, putamen, and pallidum [35].

MRI studies in SCA7 have shown diminished volumes mainly in the cerebellum and pons, while T2 images indicate hyperintensities in transverse fibers at the pons. Overall, the most consistent finding in MRI studies is pontine atrophy. Compared to other SCAs, atrophy in the pons in SCA7 seems as severe as in SCA2, and more pronounced than in SCA3 and SCA6. A recent VBM and TBSS study demonstrated bilateral

gray matter volume reductions in the cerebellar cortex and also in pre- and postcentral gyri, inferior and medial frontal cortex, inferior parietal cortex, parahippocampal gyrus, and occipital cortex [41]. This study also showed diffuse reductions in fractional anisotropy in the cerebellar white matter, brainstem, cerebellar and cerebral peduncles, midbrain, anterior and posterior internal capsule, external/extreme capsule, corpus callosum, corona radiata, optical radiations, and the occipital, temporal and frontal lobe white matter. These results confirm previous evidence of widespread damage beyond the cerebellum and the pons in SCA7.

MRI studies in SCA17 have revealed severe structural alterations in the cerebellum [42, 43]. It has been demonstrated that the extent of cerebellar neurodegeneration correlates with a variety of clinical motor features such as ataxia and extrapyramidal signs, and also with a broad spectrum of neuropsychiatric symptoms and negatively correlated with the number of CAG repeats [44]. The motor-related neurodegeneration has been shown to be progressive in a longitudinal study [45]. Recently, a task-based meta-analytic connectivity modeling and task-free resting state functional connectivity analysis showed differential functional connectivity of anterior and/versus posterior cerebellar atrophy as revealed by VBM analysis in SCA17 [46]. This study highlights the manifold connections and anterior-posterior dichotomy of the human cerebellum, providing additional valuable information about disrupted cerebellar–cerebral connections potentially underlying motor and neuropsychiatric deficits in SCA17.

Section 5: Imaging in Immune-Mediated Ataxias

Introduction This section will cover immune-mediated ataxias including gluten ataxia, anti-glutamic acid decarboxylase (anti-GAD) associated ataxia, paraneoplastic cerebellar degeneration, primary autoimmune cerebellar ataxia and post infectious cerebellitis.

Gluten Ataxia The first description of the imaging findings in patients with gluten ataxia described cerebellar atrophy in 6 out of 28 patients [47]. Subsequently Wilkinson et al. [48] used single voxel 1H MR spectroscopy of the right cerebellar hemisphere to investigate the presence of abnormal underlying cerebellar neurochemistry in patients with gluten ataxia (GA). The group demonstrated significant reduction in mean NAA concentration at short echo time and in NAA/Cho ratios at intermediate echo time in subjects compared with healthy controls. The authors concluded that cerebellar neuronal physiology is abnormal in patients with GA even in the absence of cerebellar structural deficit and that MR spectroscopy may prove a useful tool for monitoring disease. However, more recent work has indicated that the MR spectroscopy was only statistically abnormal compared to controls from the vermis which also reflects the pattern of atrophy seen, which affects the vermis earlier and more severely than the hemispheres [48, 49]. There is no published longitudinal evidence of the use of MR spectroscopy for follow up of patients with GA. In addition to the cerebellar findings, more widespread imaging abnormalities have been demonstrated amongst a population of patients presenting with celiac disease who report vague neurological symptoms [50]. Gluten ataxia appears to be associated in some individuals with accelerated white matter abnormalities compared to age-matched controls, suggesting some overlap in gluten-related neurological disease. The mechanism has not yet been elucidated.

Anti-glutamic Acid Decarboxylase Antibody Associated Ataxia Anti-GAD antibodies have been described in autoimmune diseases such as types I diabetes and multiple endocrine syndromes, and have also been found in a Stiff person syndrome and in some sporadic ataxias. It remains unclear if these antibodies are pathogenic or just a marker of multiple autoimmunity. Honnorat et al. [51] described a series of 14 patients with a cerebellar syndrome with anti-GAD antibodies, 11 of whom had late-onset insulin-dependent diabetes. The group reported that 7 of the 14 had normal MR imaging and the others pure "cerebellar atrophy", none had brainstem atrophy. In a series of six patients, Nanri et al. [52] recently described cerebellar cortical atrophy using voxel-based morphometry in all six patients with low titre GAD-antibody positive ataxia. The group also undertook SPECT imaging and reported reduced perfusion in one patient, other patients were not reported. There are no longitudinal imaging reports in the literature to assess the rate of cerebellar atrophy, correlations of clinical features to imaging biomarkers nor are there even specific reports of the patterns beyond the descriptions above. This perhaps reflects the rarity of the condition or it may be that the main imaging biomarker assessed (atrophy) is not clinically useful.

Paraneoplastic Cerebellar Degeneration Conventional, structural MRI findings are frequently normal early in the course of paraneoplastic cerebellar degeneration (PCD) but imaging can show cerebellar atrophy later in the course of the disease. Atrophy in some cases may become apparent rapidly, with reports of atrophy arising after only 1 month of symptoms [53]. De Andres [54] has reported similar florid imaging changes demonstrating T2 signal changes and cerebellar tissue swelling in keeping with underlying edema just 2 months after onset of clinical symptoms. The cerebellum subsequently became atrophic after 2 months. Choi et al. [55] reported hyperactivity of the cerebellum on brain with F-FDG-PET suggesting a very active process. However, F-FDG-PET may also show hypometabolism of the cerebellum [56]. Early and profound reductions of NAA have also been

reported on MR spectroscopy [55], which would be expected from a very active and rapid progression [7]. The same report suggested that MR spectroscopy may be a potentially useful biomarker, by showing improvement in NAA/Cr ratio following chemotherapy of the cancer but also alerting the clinician for repeat PET imaging after a fall in NAA/Cr ratio. Tumor recurrence was subsequently confirmed. If there are no clinical features to suggest a primary tumor but PCD is still suspected, PET imaging should be used as per standard investigation for an unknown primary cancer [57].

Primary Autoimmune Cerebellar Ataxia Primary autoimmune cerebellar ataxia (PACA) is a term that implies an autoimmune cause for a sporadic cerebellar ataxia that is underpinned by an appropriate HLA type such as type DQ2 or DQ8, possibly a history of other autoimmune conditions affecting the patient or their first degree relatives. There is no specific biomarker as yet, although cerebellar antibodies were found with higher frequency compared to the normal population and those patients with genetic ataxia (47 %, 3 % and 5 %, respectively) [58]. While atrophy of the cerebellum has been described in PACA, currently, there is no evidence for any specific imaging feature [59].

Post Infectious Cerebellitis Post infectious cerebellitis is normally a monophasic illness with ataxia presenting following an infection which may be subclinical. Imaging plays a modest role in diagnosis; T2 signal change of the cerebellum is widely documented [60, 61] but structural MRI findings maybe normal if patients are imaged early in the course of the illness [62, 63]. While SPECT perfusion has been reported as a potential diagnostic biomarker in the course of the illness, reports vary with both increased and decreased perfusion demonstrated alongside normal MR appearances of the cerebellum [62, 63]. The pattern of cerebellar involvement is variable, though with the Purkinje cell a frequent immunological target in immune-mediated ataxia of which nature there is often a predominant cerebellar cortical volume as tends to be found in other immune ataxias [59]. Most patients make a full recovery with no residual imaging abnormalities. In a minority, there is subsequent evidence of cerebellar atrophy, sometimes with evidence of progression. This latter group, however, may fall into the category of primary autoimmune cerebellar ataxia.

Section 6: Radiological Biomarkers of Cerebellar Alteration in Dementia

The cerebellum has traditionally been seen as a brain area limited to the coordination of voluntary movement, gait, posture, speech, and motor functions. However, there are increasing evidence proving that the cerebellum is implicated in processes associated with the control of cognition, behavior, and psychiatric illness [64, 65]. Moreover, the fact that the cerebellum is reciprocally connected to a broad range of limbic structures including the amygdala and hippocampus, as well as the cerebral cortex including the prefrontal areas, provides a strong neuroanatomical argument in favor of cerebellar involvement in cognition regulation [66].

Functional neuroimaging studies show that the cerebellum is involved in multiple cognitive functions, including working memory and attention [67–69]. Damage to the cerebellum, particularly the posterior lobes and vermis, is consistently associated with cognitive deficits [69–72]. In young, healthy adults, some studies have found that cerebellar size is associated with individual differences in cognitive ability [69, 73]. The cerebellum is relatively vulnerable to atrophy occurring with aging and cognitive domains known to involve the cerebellum, for example, working memory, are vulnerable to decline with aging [67, 74]. In this context, some researchers have showed an interest in supratentorial atrophy [68, 75–77]. Although population-based studies have widely investigated structural properties of the cerebrum, the cerebellum has received little attention [78].

Dementias constitute a heterogeneous group of diseases that share cognitive impairment of organic etiology. Although several causes and pathophysiological mechanisms underlie the clinical presentation of different types of dementia, neuroimaging studies have confirmed some common findings such as atrophy of certain brain structures or even global brain atrophy and progressive impairment of different cognitive domains [65]. In Alzheimer's Disease (AD), for example, temporal lobe volume reduction is observed even at early stages of the disease, and hippocampal reduction can be observed before the first symptoms [65].

Cerebellar changes can occur in several types of dementia [65, 79–82]. Generally, these findings are organized in neuroimaging secondarily, on the other hand, some cerebellar diseases may also present with dementia. Regardless of place of primary amendment, each disease shows morphological alterations of the cerebellum in a particular way. Besides, in neuroimaging studies, the greatest difficulty in assessing cerebellar changes is that this structure is generally used as a control, in other words, it is considered as a structure free of the condition to be compared to cerebrum alterations. Therefore, the study of cerebellar changes in dementia is a new perspective in understanding the neurodegenerative diseases and enables a new way of understanding its pathophysiology, symptoms, and treatment, and prognosis mainly. Additionally, since the cerebellum participates in the regulation of motor activity, working memory, attention, and executive functions, the changes suffered by it may be related to loss of functionality, one of the factors related to the prognosis of dementia.

In previous studies about cerebellar abnormalities in different types of dementia, the most relevant finding is diaschisis, that is the cerebellar hypoperfusion or hypometabolism related to the atrophy of superior structures and is commonly observed at late stages of disease [83–85]. The main hypothesis suggesting the implication of the cerebellum in dementia invokes a possible role for diaschisis [65, 75–77], however, it was demonstrated that cerebellar volume reductions can be observed even at early stages of the disease [65]. Moreover, there are reports that secondarily affected regions could present mild atrophy and no histopathological changes [76]. Possible reasons for cerebellar volume reductions in dementia include vascular factors, toxins (e.g., alcoholic dementia) [65, 75, 76, 80], and normal aging [75].

In structural MRI in AD, cerebellar volume is reduced [65, 77, 83, 86] and shows microstructural changes [84]. There is gray matter density reduction in AD compared to healthy controls as an independent variable [84]. Cerebellar lobes volume, posterior cerebellar lobes, and vermal volume reduction are the main findings in AD patients when compared to healthy controls, and that this atrophy is associated with poorer cognitive performance in AD [77]. The volume reduction is an independent variable; besides, reduction in superior structures are present [72]. The volume reduction is more evident in the late stages of disease. In addition, right cerebellar hemisphere and vermis volumes have a negative correlation with the functional activities [65].

In functional and molecular research, usually, the cerebellum is often used as a control structure, since this structure is free of neurofibrillary and β-amyloid pathology (except in very late states). A significant reduction of blood flow in cerebellum was observed in patients with AD compared to healthy controls [85]. Other groups observed that the glucose metabolism in the cerebellum was significantly lower in patients with AD comparing to healthy controls and this reduction correlated with MMSE [87]. Using functional MRI (fMRI), Vidoni and colleagues [88] observed that individuals without dementia exhibited greater activation in accessory motor regions supplementary motor area and cerebellum compared to those with AD.

In other types of dementia, cerebellum morphology is not assessed frequently and few data are available. In vascular dementia, cerebellar changes are diverse and brain atrophy can occur directly by vascular lesion in the cerebellum or secondary to cerebrum atrophy [89]. Studies have already found the fact that after stroke, the cerebellum suffered from reduction in metabolism and blood flow in the cerebellar hemisphere contralateral to a destructive cerebral lesion [79, 90]. But there is a particular change in subcortical vascular dementia that present with cerebellar volume reduction, and the number of subcortical lacunes correlates with cerebellar atrophy [91].

There is reduction in the gray matter of the cerebellum in frontotemporal dementia, and there is hypometabolism in the cerebellum together with hypometabolism in the prefrontal cortex, thalamus, parietal-occipital white matter, lenticular nucleus of the basal ganglia, and pons [80, 91]. After a working memory task, frontal regions in patients with FTD showed less linear activation, but the cerebellum shows a stronger increasing response in FTD [78], suggesting a compensatory mechanism.

In Parkinson disease (PD) there is gray matter volume decrease in the right quadrangular lobe and declive of the cerebellum in subjects with tremor compared with those without. Increased activation of the cerebellum in PD appears not only during motor execution, but also during the motor learning process [81]. But the patients with PD in a gait-induced task have hypoactivation in the left medial frontal area, right precuneus and left anterior lobe of the cerebellar hemisphere, but hyperactivity in the left temporal cortex, right insula, left cingulate cortex, and cerebellar vermis [90].

In Huntington's disease (HD), the anger recognition deficit was correlated with atrophy of selected hemispheric and vermal regions of the cerebellum in addition to the common findings of basal ganglia including the caudate nuclei, putamen, and globus pallidus [82]. Furthermore, cerebellar volume reductions of the HD patients were associated with longer disease duration and greater functional impairment [82].

Fahr's disease (FD) is characterized by sporadic or familiar idiopathic calcification of the basal ganglia, dentate nuclei of the cerebellum, and centrum semiovale, mainly presenting with movement disorder, dementia, and behavioral abnormalities [92, 93]. In Fahr's syndrome brain CT, the most frequent site of calcification is in basal ganglia, and MRI shows atrophy in parietotemporal regions. But deposits may be present in the cerebellum [92, 93].

Finally, Creutzfeldt-Jakob Disease (CJD), that is the most common prion disease, characterized by a rapidly progressive multifocal neurological dysfunction, myoclonic jerks, and a terminal state of global severe cognitive impairment [94]. Magnetic resonance imaging of the brain may have an important role in the diagnosis of disease [95]. Typical MRI findings in CJD patients consist of hyperintense signals in the cortical ribbon, basal ganglia, and the thalamus on diffusion-weighted images (DWI) and fluid-attenuated inversion recovery (FLAIR). Despite the intense neuropathological involvement of the cerebellum in CJD [96] and presence of cerebellar symptoms [97, 98], it is commonly negative in imaging studies [99, 100]. More recently, Cohen et al. found that apparent diffusion coefficient values are elevated in cerebellar structures [94]. There is increased cerebrospinal fluid volume in the posterior cranial fossa suggesting cerebellar atrophy. The author proposed this atrophy as a radiological hallmark of cerebellar pathology in CJD [94]. In Sporadic Creutzfeldt-Jakob disease (sCJD), there is a hypometabolism in the cerebellum measured by SPECT or PET and the presence of

hyperintensities on MRI. In familiar form, there is reduction of metabolism as in sCJD [79].

Another type of prion diseases could present without abnormalities, atrophy, or another small findings. For example, the Gerstmann–Sträussler–Scheinker syndrome (GSS) is characterized by slowly progressive cerebellar ataxia accompanied by cognitive impairment, spastic paraparesis, and extrapyramidal signs. In this disease, there is decrease in the NAA/Cr ratio in the frontal lobe, cerebellum, and putamen even in the absence of other abnormal imaging results [100].

Based on preliminary findings, there is evidence that the cerebellum could be impaired in dementia. Although cerebellar changes accompany similar changes in the cerebrum, they cannot be considered as an isolated factor only. We have hypothesized two possible ways in which cerebellar volume and function may change: (1) cerebellar impairment could be secondary to cerebral volume reduction, or (2) cerebellar impairment could be evident prior to cerebral impairment and could be related to other factors. These hypotheses suggest that cerebellar volume reductions can be considered as a risk factor for later dementia onset. As the cerebellum participates in coordination, gait, and in some cognitive functions (as executive), its impairment could be related to the outcome and mortality rates in dementia [101]. Therefore, a better understanding of the role of the cerebellum in dementia could offer new possibilities for prevention and rehabilitation.

Section 7: Markers of Cerebellar Alteration in Autism Spectrum Disorder

Markers of Cerebellar Alteration in Autism Spectrum Disorder Autism spectrum disorder (ASD) is an early-developing disorder marked by impairments in social communication and restricted and repetitive interests [102]. The cerebellum of individuals with ASD often manifest marked anomalies. Recent conceptions of the cerebellum link this structure, via its robust afferent and efferent connections, to nearly every major neural system—including prefrontal, posterior parietal, temporal, and limbic structures—and to a broad suite of functions [103] including many known to be abnormal in ASD. Early cerebellar abnormalities in ASD could contribute to the altered developmental trajectories and heterogeneity evident in this disorder.

Cellular and Molecular Findings Postmortem studies in patients with ASD have consistently documented reduced Purkinje cell (PC) density in the hemispheres and vermis [104]. This reduction may be greatest in Crus I and II [103], regions of the so-called "cognitive cerebellum" with linkages to non-motor cortical association regions. Dysregulation of chemicals involved in cellular migration (Reelin) and apoptosis (Bcl-2) has been found in the cerebellum of individuals with ASD [105], providing one potential explanation for PC reductions.

Genetics of the Cerebellum in ASD Work has implicated engrailed 1 and 2 (EN1 and EN2) as potential candidates for cerebellar pathology: Human EN2 maps to a region of chromosome 7 that has been linked to ASD [106], and EN2 mouse mutants display relevant ASD-like features such as PC reductions [107] and reduced exploratory behaviors [108]. Another genetic link may be MET (transmembranar receptor tyrosine kinase of the hepatocyte growth factor/scatter factor), which is implicated in neuronal development in the cerebellum [109], and has been implicated in genetic analyses of 7q in autism families [110].

Gene by environmental interaction could also result in PC loss due to prenatal neuro-inflammatory reactions (i.e., neuroglial activation) [111]. In mouse models, prenatal viral infections result in dysregulation of myelin-associated genes in the cerebellum, which appears to lead to alterations in cerebellar white matter [112, 113].

Volumetric Findings Courchesne and colleagues [114] have proposed that within the cerebellum, there may be in ASD early overall cerebellar enlargement with decreased or arrested growth during childhood. In contrast to the development of the cerebellar hemispheres, the superior posterior vermis (vermal lobules VI–VII) may be significantly smaller in a subset of autistic patients (for meta-analysis [115]). Cerebellar vermis has connectivity with limbic and paralimbic regions, and activity in vermis VI–VII is associated with emotional processing in nonclinical samples [104]. Volumetric data on the other vermal lobules (I–V, VIII–X) are, however, inconsistent, and vermal growth trajectory in ASD is unclear. Trajectories of different vermal lobules may vary, with I–V and VI–VII, but not VIII–X, "catching up" by adolescence. As yet undetermined is the implication of altered and different trajectories within specific cerebellar lobules.

Cerebello-Cortical Connectivity Contemporary theories of cerebellar function suggest that cerebellar neuronal operations are uniform, but that their outcomes differ based on highly specific patterns of cerebello-cortical connectivity. Thus, fully understanding the nature and downstream implications of cerebellar disruptions depends on robustly characterizing cerebello-cortical connectivity in ASD as well as disruptions to the cerebellum in isolation. A few investigations in this domain suggest atypical functional [116] and anatomical connectivity [117]; however, this area is ripe for further research.

Cerebellum and Behavior in Autism In ASD, cerebellum volume and white matter integrity have been shown to be associated with performance IQ [118], repetitive behaviors [119, 120], social behaviors [116], and symptom

discrepancies [121]. However, not all reports find behavioral relations [122]. Resolving the inconsistency across reports, in terms of whether these relations do exist and in which domains, may necessitate greater attention to how these complex behaviors might be linked to topographically varying patterns of cerebellar connectivity, as well as how these relations might covary with methodological considerations and variability in sample characterization.

Cerebellar Treatment Targets in ASD? Although the cerebellum has been identified as a potential region of interest for ASD, it has received little attention as a potential therapeutic target [103]. One potential pharmacological target is cerebellar GABAergic dysfunction, which has been repeatedly demonstrated in ASD [112]. The GABA B receptor agonist, arbaclofen, has been reported to be helpful in preliminary trials for irritability and social withdrawal in autism, and is moving forward in clinical trials [123]. Another avenue may be calcium channelopathies. Increased cerebellar activity of the enzymes Na(+)/K(+)-ATPase and Ca(2+)/Mg(2+)-ATPase in ASD could represent a compensatory response to increased intracellular calcium concentration, representing a potential drug development target [124].

Section 8: Structural and Functional Neuroimaging in Autosomal Recessive and X-Linked Ataxias

Autosomal Recessive Ataxias Autosomal recessive ataxias represent a very heterogenous and relatively numerous group of diseases which can be variably classified according to clinical features, including age of onset, disease progression rate and associated signs, neurophysiology findings or underlying genetic abnormality (Table 2) [125]. Neurophysiological findings and several characteristic or pathognomonic laboratory findings can help in the differential diagnosis of autosomal recessive ataxias, whereas the most common MRI finding, namely cerebellar atrophy, is nonspecific [125]. However, taking into consideration the pattern of inheritance which implies in some cases a less evident familiar transmission of the disease as compared to autosomal dominant ataxias, it is important to be aware that some autosomal recessive ataxias show typical MR imaging features which can serve as crucial diagnostic biomarkers in the single patient (Fig. 2 and Table 2). These include: "molar tooth" sign in Joubert syndrome and related disorders (ciliopathies) [126, 127]; a pattern of spinal atrophy combined with symmetric high signal in the lateral and posterior columns of the cervical spinal cord in Friedreich ataxia [1]; cortical cerebellar atrophy combined with foci of hypointensity on T2*-weighted gradient echo images corresponding to capillary telangectasias in ataxia telangectasia [128]; atrophy of the superior cerebellar vermis, a bulky pons exhibiting T2-hypointense stripes corresponding to the corticospinal tracts and medial leminsci, thinning of the corpus callosum and a rim of T2-hyperintensity around the thalami in autosomal recessive spastic ataxia of Charlevoix-Saguenay [129]; symmetric high signal in the hilum of the dentate cerebellar nuclei on T2-weighted images in cerebrotendineous xanthomatosis (CTX) [130].

Quantitative MR and nuclear medicine techniques have been successfully used for physiopathological characterization of some autosomal recessive ataxias, namely Friedreich's ataxia (FRDA), ataxia with oculomotor apraxia type 2 (AOA2), CTX and Niemann–Pick type C (NPC) disease.

FRDA is the most common autosomal recessive ataxia which is now readily diagnosed by demonstration of expanded GAA trinucleotide repeat in both the alleles of a gene encoding a mitochondrial protein named "frataxin". Conventional MR imaging shows atrophy of the cervical spinal cord and medulla and symmetric T2 high signal in the lateral and posterior WM columns of the spinal cord [1]. More importantly, some quantitative MR measures were reported to be correlated with severity of clinical impairment. These include reduced thickness and increased proton diffusion of the cerebellar WM and superior cerebellar peduncles [131–134]. In addition, a measure of the integrity of the superior cerebellar peduncles, namely magnetization transfer ratio, correlated with the number of GAA triplets in the larger repeat size in a recent study [135]. FDG-PET demonstrates a distinctive diffuse pattern of increased glucose metabolism in the brain of FRDA patients with mild to moderate clinical impairment [136]. Conversely, in patients with more severe deficit, a normal pattern or decrease of glucose metabolism in the cerebral cortex, the cerebellum, and the brainstem, is observed [136].

MRI in AOA2 shows a nonspecific cortical cerebellar atrophy pattern associated with stroke-like cerebral lesions, whereas proton MR spectroscopy shows lower *N*-acetyl-aspartate (NAA) consistent with neuronal loss/dysfunction in the cerebellar vermis and hemispheres, increased myo-inositol indicative of gliosis in the pons and vermis and decreased glutamate in the vermis [137]. The cerebellar NAA concentration correlates with severity of clinical cerebellar deficit.

In CTX, a decrease of NAA combined with increase of lactate was observed in the supracallosal brain, which correlated with clinical disability, and in the deep cerebellar WM [138].

In NPC patients, thinning of the corpus callosum is correlated with duration of the disease and measures of clinical severity [139]. Moreover, a recent morphometry study [140] indicated that NPC patients shows a significant reduction in both gray and white matter cerebellar volumes and that volume loss is correlated with saccadic gain and ataxia measures, but not with symptom duration or severity. In a proton spectroscopic imaging study of NPC disease, NAA/creatine was significantly decreased in the frontal and parietal cortices, centrum semiovale and caudate nucleus, whereas choline/

Table 2 Genetic, clinical, laboratory and conventional MRI in most common recessive ataxias [modified from Anheim et al. (ref. 125)]

Disease	Gene and protein	Age at onset	Key symptoms in addition to cerebellar ataxia	Laboratory findings	Conventional MRI
Cerebellar ataxias with pure sensory neuropathy					
FRDA	*FXN* frataxin	2-60 mean 16	Bilateral Babinski sign, scoliosis, square-wave jerks	GAA triplet repeat expansion in intron1 of *FXN* gene	Spinal cord and bulbar atrophy, symmetric T2 high signal in posterior and lateral columns of the spinal cord
AVED	*TTPA* alpha-tocopherol transfer protein	2-50 mean 17	Bilateral Babinski sign, scoliosis, retinitis pigmentosa	Decreased serum level of vitamin E	Spinal cord atrophy
Cerebellar ataxia with sensorimotor axonal neuropathy					
AT	*ATM* Ataxia Telangectasia mutated	2–3	Conjuctival telangectasias, dystonia, chorea, susceptibility to infections and cancer	Elevated serum Alpha-feto-protein, immunoglobulin deficiency, specific karyotype	Cerebellar atrophy brain T2 hypointense dots
AOA 1	*APT* aprataxin	1–20 mean 7	Oculocephalic dissociation, chorea, dystonia	Elevated serum LDL cholesterol, low serum albumin	Cerebellar Atrophy
AOA2	*SETX* senataxin	7–25 mean 15	Oculocephalic dissociation, chorea, dystonia	Elevated serum Alpha-feto protein	Cerebellar Atrophy
ARSACS	*SACS* sacsin	Up to 12 mean 2	Spastic paraparesis, distal amyotrophy to 4 arms, pes cavus, scoliosis		Atrophy of superior vermis, thinned corpus callosum, T2 hypointense stripes in a bulky pons, T2 hyperintense rim around the thalami
CTX	*CYP27* Sterol27 hydoxylase	Childhood	Sensory neuropathy, spasticity	Elevated serum cholestanol	Cerebellar atrophy, cerebellar and cerebral WM T2 hyperintensity
Cerebellar ataxia without neuropathy					
JSRD	10 causative genes encoding for proteins of the primary cilium (see ref [126])	Neonatal period	Hypotonia, oculomotor apraxia, facial dysmorphism, irregular neonatal breathing, cognitive impairment, involvement of kidneys, liver, eyes		"Molar tooth", vermal hypoplasia, enlarged IV ventricle and posterior fossa
ARCA1	*SYNE1* Spectrin	17–46 mean 32	Pure ataxia		Cerebellar atrophy
ARCA2	*ADCK3* Aarf-domain containing Kinase 3	1–11 mean 4	Mental retardation, myoclonus, epilepsy, stroke like episodes	Elevated serum lactic acid, decreased coenzyme Q10	Cerebellar atrophy, stroke-like lesions
NPC	*NPC1* NPC1 *NPC2* NPC2	2–30	Vertical supranuclear ophthalmoplegia, dystonia, cognitive impairment	Skin biopsy findings	Variable cerebral and cerebellar atrophy

AOA1 ataxia with oculomotor apraxia type 1; *AOA2* ataxia with oculomotor apraxia type 2; *ARCA1* autosomal recessiva cerebellar ataxia type 1; *ARCA2* autosomal recessive cerebellar ataxia type 2; *ARSACS* autosomal recessive spastic ataxia of Charlevoix-Saguenay; *AT* ataxia telangectasia; *AVED* ataxia with vitamin E deficiency; *CTX* cerebrotendineous xanthomatosis; *FRDA* Friedreich's ataxia; *JSRD* Joubert syndrome and related disorders (ciliopathies); *NPC* Niemann–Pick type C

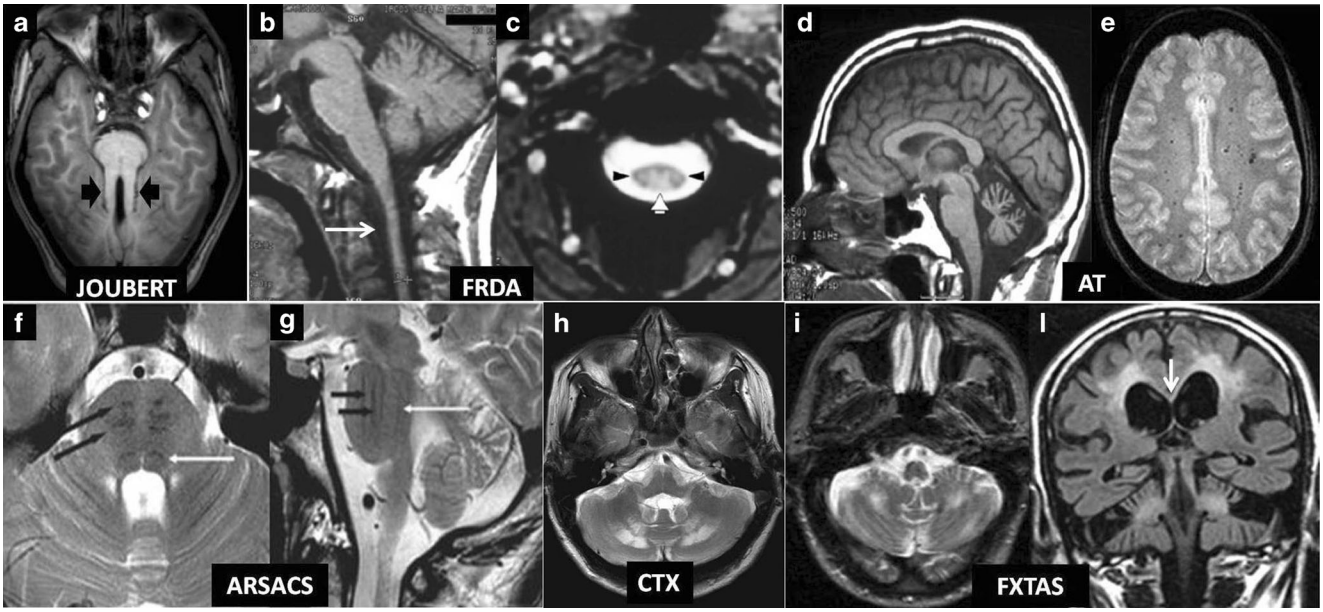

Fig. 2 **a**–**l** Diagnostic biomarkers of recessive and X-linked inherited ataxias on conventional MRI. Axial T1 weighted image (**a**) showing symmetrically thickened and parallel oriented superior cerebellar peduncles (*black arrowheads*) creating the "Molar Tooth" sign characteristic of Joubert syndrome and related disorders. Note also the small and dysmorphic vermis. Sagittal T1-weighted image (**b**) shows atrophy of the medulla and cervical spinal cord (*arrow*) in a case of Friedreich ataxia (FRDA). Axial T2*-weighted gradient echo image (**c**) confirms the decreased size of the cervical cord cross-section in the same disease and demonstrates symmetric hyperintensity of the posterior (*white arrowhead*) and lateral (*black arrowheads*) columns of the spinal cord (both images reprinted with permission from ref. [1]). Sagittal T1-weighted image (**d**) demonstrates widened vermian sulci in a patient with ataxia telangectasia (AT) consistent with a macroscopic pattern of cerebellar cortical atrophy (image reprinted with permission from ref. [1]). Axial T2*-weighted gradient echo image (**e**) demonstrates multiple hypointense dots in the centrum semiovalis WM consistent with capillary telangectasias in another patient with AT (image reprinted with permission from ref. [128]). Axial (**f**) and sagittal (**g**) T2-weighted images in a patient with recessive spastic ataxia of Charlevoix-Saguenay (ARSACS) show characteristic low signal intensity stripes (*black arrows*) corresponding to the corticospinal tracts in a bulky basis pontis. The *white arrow* in **f** and **g** indicates the hypointense medial lemniscus (both images reprinted with permission from ref. 129). Axial T2-weighted image (**h**) shows characteristic symmetric hyperintensity of the peridentate cerebellar WM in a patient with cerebroendineous xanthomatosis (image reprinted with permission from [130]). Axial T2-weighted image (**i**) in a patient with Fragile X-associated tremor ataxia syndrome (FXTAS) shows symmetric hyperintensity of the cerebellar WM which is accompanied in a coronal T2-weighted FLAIR image (**l**) by symmetric extensive areas of hyperintensity of the cerebral WM and of the splenium of the corpus callosum (*arrow*). *Joubert* Joubert syndrome and related disorders; *FRDA* Friedreich's ataxia; *AT* ataxia telangectasia; *ARSACS* autosomal recessive spastic ataxia of Charlevoix-Saguenay; *CTX* cerebrotendineous xanthomatosis; *FXTAS* Fragile X-associated tremor ataxia syndrome

creatine was significantly increased in the frontal cortex and centrum semiovale [141]. Significant correlations were found between clinical staging scale scores and these proton spectroscopy abnormalities.

Although overall, the above findings suggest a role of MR or nuclear medicine measures as progression and surrogate biomarkers of recessive ataxias, to date, these potentials of neuroimaging techniques have not been proven in longitudinal studies.

X-Linked Ataxias The most common form of X-linked ataxia is the Fragile X-associated tremor ataxia syndrome (FXTAS) [142, 143]. In 57 % of FXTAS cases, there is familial history of mental retardation affecting a boy due to full (in excess of 200) expansion of a CGG triplet in the fragile X mental retardation 1 gene [143]. Accordingly, FXTAS is typically diagnosed in the grandfather of a boy with fragile X mental retardation [142, 143] and is associated with a reduced (in the 55–200 range) CGG expansion of the same gene. Clinical features of FXTAS include a progressive syndrome characterized mainly by tremor, cerebellar ataxia, peripheral neuropathy, and cognitive dysfunction [143]. MRI is an important diagnostic biomarker of FXTAS which can present as a sporadic condition also in women [142, 143]. In particular, it demonstrates characteristic symmetric areas of T2 hyperintensity in the peridentate WM and middle cerebellar peduncles combined with symmetric signal changes in the periventricular cerebral WM and in the splenium of the corpus callosum (Fig. 2). There is a diffuse atrophy of the brain in the supra and infratentorial compartments, but the oval shape of the basis pontis is preserved [144]. Signal changes in the peridentate regions correlate with severity of ataxia, whereas signal changes in the splenium of the corpus callosum mark disease progression [143]. In addition, a voxel-based morphometry study indicated that gray matter loss in the vermis correlates with severity of motor symptoms, atrophy of the left amygdala correlates with increased levels of obsessive–compulsiveness and depression, and atrophy of the left inferior

frontal cortex and anterior cingulate cortex correlates with poor working memory performance [145].

SPECT studies have revealed decreased uptake of the dopamine transporter and postsynaptic D2 receptors in the striata, accounting for the extrapyramidal symptoms often observed in patients with FXTAS [143, 144, 146].

To date, no longitudinal study has addressed the potentials of the above MR and nuclear medicine findings as progression or surrogate biomarkers of FXTAS.

Section 9: Metabolic Cerebellar Ataxia (In Children)

A growing number of metabolic disorders that can entail cerebellar ataxia in childhood have been identified. These disorders usually implicate one or several metabolic pathways and are mainly characterized by: sporadic or hereditary genetic default causing enzymatic dysfunction, multisystemic impairments, variable age onset, nonspecific clinical expression, and an intermittent or progressive ataxic expression [147]. These disorders are often autosomic recessive but not exclusively. The majority of (mostly hereditary) metabolic cerebellar ataxia results from: alterations of amino acids (maple syrup urine disease, L-2 hydroxyglutaric acidemia, isovaleric acidemia), lysosomal (Krabbe's disease, metachromatic leukodystrophy, Niemann–Pick disease type C, hexosaminidase A deficiency), peroxysomal (adrenoleucodystrophy, adrenomyeloneuropathy, Refsum disease) and glycosylation metabolisms, urea cycle, lactic acidosis (Leigh's disease), leukodystrophies (Canavan's, Alexander's and hypomyelination disorders such as: Pelizaeus–Merbacher diseases, Pol-III related leukodystrophies: 4A, Cockayne syndrome, 18q-syndrome, fucoscidose, hypomyelination with atrophy of the basal ganglia and the cerebellum), mitochondropathy (MELAS, Kearns–Sayre syndrome), defects in gene encoding myelin protein and some miscellaneous troubles such as Wilson disease, Menkes disease, cerebrotendinous xanthomatosis, infantile neuroaxonal dystrophy, leukoencephalopathy with vanishing white matter, megalencephalic leukoencephalopathy with subcortical cysts and deficiencies in: biotine/biotinidase/holocarboxylase synthetase, sulfite oxidase and molybdenum, vitamin E or apolipoprotein B, for example [147–150].

Aside from clinical symptoms, the diagnosis of such (often rare) metabolic troubles relies principally on biochemical analysis of abnormal metabolites within urine, blood, cerebrospinal fluid or cellular culture (fibroblast), and mutation analysis of specific genes. Magnetic resonance imaging (MRI) allows further morphological and biochemical characterization of such diseases.

Structural neuroimaging can detect numerous but heterogeneous subcortical or/and periventricular, supra- or/and infratentorial abnormalities in gray and white matter. The most affected brain structures are: cerebral cortex (thinning, atrophy), white matter (delayed myelination, cysts and abnormal FLAIR/T2-hyperintensity often due to demyelination), basal ganglia, especially the putamen (T2-hypointensity, atrophy, calcium deposits), thalamus, and some brainstem nuclei and tracts, while the most frequent but unspecific abnormality is leukoencephalopathy. It is noteworthy that white matter alteration can sometimes be a side effect of Wallerian degeneration accompanying gray matter abnormalities. In particular, T2-hyperintensity in white matter occurs during leukodystrophies, lysosomal and peroxisomal disorders, and mitochondropathy. Microstructural disorganization of the white matter, in particular caused by myelin injury can be assessed by diffusion-weighted imaging and quantified by the apparent coefficient of diffusion, radial or axial diffusivity, or fractional anisotropy. Other MRI sequences such as magnetic transfer magnetization, T1 and T2 relaxometry or tractography may also provide interesting information concerning white matter injury or recovery [148], while voxel-based morphometry and double-inversion recovery will give important information about gray matter. Contrast-enhancement in white matter or cerebellum is inconstant and is mainly observed in adrenoleukodystrophy and in Alexander disease, respectively. Concerning the cerebellum, a wide range of abnormalities has been observed from atrophy/hypoplasia, the most usual described sign, to T2-hyperintensity white matter or abnormal deep cerebellar nuclei. Although some differential regional patterns can be described in terms of anatomical localization or morphology, no one proves to be specific of a particular disease (diagnostic radiomarkers).

^{1}H MR spectroscopy (MRS) can usefully complement MRI morphological data for diagnostic orientation [149, 151]. Lactate (anaerobic metabolism; doublet peak at 1.33 ppm) is commonly detected in mitochondropathies because of the disruption of the electron respiratory chain, but also in neuronal ceroid liposfuscinosis. More specific metabolites, and thus potential radiomarkers, can be also identified such as: galacticol (3.67/3.74 ppm) in galactosemia type 1, phenylalanine (7.37 ppm) in phenylketonuria, branched-chain amino acids and ketoacids (0.9 ppm) in maple syrup urine disease, increased *N*-acetyl-aspartate (NAA; 2.02 ppm) in Canavan's disease. Moreover, decreased NAA/choline ratio below 5.0 might predict progression of X-linked adrenoleukodystrophy (evolution biomarker) [152]. Combining morphological and spectroscopic disease characteristics may help to reach a diagnosis. For instance, mitochondropathies (including Leigh's disease) can be suspected and discriminated by differential patterns of T2-hyperintensities and atrophy (subcortical white matter, basal ganglia, brainstem, colliculi, cerebellum including dentate nuclei, and less often thalami), lactate increase and stroke-like lesions [153]. Association of cerebellar atrophy and high lactate peak within the cerebellum seems strongly in favor of mitochondropathy-related cerebellar ataxia [154].

Therefore, the great heterogeneity and the nonspecificity of MR data, the existence of overlapping MRI expression of different diseases, the changing aspect of the brain lesions with time and the small sample size of patient group due to the rarity of these diseases hamper to define the role of these potential radiomarkers for diagnosis and evolution assessment. However, some strategies, called pattern-recognition approach (PRA), have been developed to reduce progressively the list of possible diagnoses on the basis of well-defined anatomical criteria, which can be secondarily complemented by biochemical data [148, 155]. For example, PRA will successively consider: gray and/or white matter involvement, subcortical and/or deep white matter involvement, symmetric or asymmetric lesions, basal ganglia and/or thalamus lesions, brainstem and cerebellar involvement, and so on [149]. This decision tree leads to group patients in distinct categories of better-circumscribed (but still too wide) diagnosis. Such classification can also benefit from advanced statistical methods. Steenweg et al. [155] classified successfully some hypomyelination disorders by applying multivariate and unsupervised hierarchical clustering to MRI characteristics of patients, such as T2-hyperintensity in white matter, basal ganglia, or pons, T2-hypointensity in the pallidum or cerebellar atrophy, for instance. It can, thus, be speculated that definition of such patterns of metabolic-related structural and biochemical abnormalities, enriched by new unconventional MRI sequences with possible quantification of MRI parameters and even by refined statistical analyses such as principal component analysis or hierarchical clustering, will enable to diagnose more and more specifically and unequivocally cerebellar metabolic ataxia in the future.

Section 10: Sporadic Adult-Onset Ataxia of Unknown Etiology and Multiple Systems Atrophy

Multiple system atrophy (MSA) is a rare, sporadic, progressive, neurodegenerative disorder with a late onset (around 50 years). Clinical presentation mainly combines parkinsonism (akinesia, rigidity, tremor, postural instability), cerebellar ataxia (gait, speech and limb ataxia and gaze-evoked nystagmus), autonomic dysfunction (genito-urinary impairments, orthostatic hypotension), pyramidal syndrome and REM-sleep behavior disorder. MSA can be divided into MSA with parkinsonism predominance (MSA-P) and MSA with predominant cerebellar ataxia (MSA-C) [156, 157]. Cognitive and psychiatric troubles have been reported in MSA-C. Histopathological studies have identified distinctive oligodendroglial alpha-synuclein fibrillar intracytoplasmic inclusions associated with gliosis, and neuronal loss (apoptosis) within basal ganglia, cerebellum, pons, bulbar olivary nucleus and spinal cord (intermediolateral column). Neuroimaging may help to diagnose MSA and to characterize MSA-related anatomical abnormalities. The main MRI features of MSA (especially MSA-C) are: variable atrophy of cerebellum, middle cerebellar peduncle, pons, and putamen. Atrophy is also observed in frontal and insular cortices, medial part of the corpus callosum, and, at follow-up, in thalamus and caudate nucleus [158, 159]. More suggestive but not pathognomonic signs include: a cruciform T2 hyperintensity in the pons ("hot cross bun") although found in other types of ataxia such as SCA, dorsolateral putaminal rim T2 hyperintensity (with increased MD in DTI), middle cerebellopeduncular and putaminal hypointensity. Postmortem MR-pathological correlations have established that: (1) cerebellar white matter atrophy was more severe than gray matter atrophy, (2) white matter T2 hyperintensities reflect demyelination and gliosis, and (3) dentate (and putaminal) hypointensities is linked to iron/ferritin deposition [160, 161]. T2-relaxometry can detect increased relaxation rate R2 of morphologically normal putamen in MSA-C [162]. Several microstructural alterations within infra- and supratentorial structures have been determined using diffusion imaging and quantified by measures of ADC, MD, and FA. For instance and interestingly, the middle cerebellar peduncle displays: increased ADC and reduced FA (like the cerebellum) which is correlated with the Barthel index, rating the performance of daily activities and disease duration. DTI can detect early FA decrease and MD increase in pontine transverse and longitudinal fibers implicated in the "hot cross bun" but before its morphological expression [163]. DTI can also detect transverse pontocerebellar fibers and corticospinal degeneration more easily than T2 sequence [164]. Moreover, increased ratio of myo-inositol/creatine evaluated with ^{1}H MR spectroscopy in the pons and medulla would be correlated with MSA-C severity. Increased cerebellar lactate peaks measured in ^{1}H MR spectroscopy could contribute to distinguish SCA2 from MSA-C [165]. Moreover, SPECT and PET data point out possible: (1) hypometabolism in cerebellum, middle cerebellar peduncle, pons and putamen, (2) presynaptic nigrostriatal dopaminergic denervation, and (3) alteration of the cholinergic (Ch5–Ch6) projections from pedunculopontine and laterodorsal tegmental nuclei to the thalamus correlated with motor and disability impairments [166, 167]. In conclusion, no MRI abnormality seems to be specific of MSA-C. A combined MRI and dopamine receptor imaging with [123I]-IBZM-SPECT reported a more severe cerebellar and brainstem atropy with MSA-C than MSA-P, while the loss of dopamine receptor was identical in both groups [168]. However, a combination of several signs such as cerebellar and pons atrophy and hypometabolism, "hot cross bun" and putaminal alterations may be very suggestive of MSA-C (diagnosis radiomarker). 3D-based MRI morphometry of the putamen and of the cerebellum can be used as a marker of disease progression [169].

Sporadic adult-onset ataxia of unknown etiology (SAOA) is characterized by a progressive ataxia occurring after 20 years (most often around 50 years) with a male preponderance and negative family history and without any causative genetic or acute disorders [170]. Clinical features can also include, more inconstantly, a pyramidal syndrome, polyneuropathy (one third of patients), and mild cognitive, autonomic, and motor impairments. Some proprioceptive

deficits are frequently observed such as decreased vibration sense, or decreased/increased/absence of ankle reflexes. SAOA is accompanied by atrophy affecting mostly the cerebellar gray matter (especially superior vermis, and likely linked to Purkinje cell loss and gliosis), the white matter of the middle cerebellar peduncle and the outer edge of the pons. FDG-PET also revealed cerebellar, brainstem, and cerebral cortical hypometabolism. MRI pattern of the brain can be very close between SAOA and MSA [162]. However, brainstem atrophy is more prominent in MSA patients than in SAOA patients [171]. Moreover, in comparison with SAOA, MSA-C shows specific decreased regional blood flow in brain areas such as caudate tail, and lingual and fusiform cortices, and in the pons.

Conflict of Interest All authors declare no conflict of interests.

References

1. Mascalchi M, Vella A. Magnetic resonance and nuclear medicine imaging in ataxias. Handb Clin Neurol [Rev]. 2012;103:85–110.
2. Currie S, Hadjivassiliou M, Craven IJ, Wilkinson ID, Griffiths PD, Hoggard N. Magnetic resonance imaging biomarkers in patients with progressive ataxia: current status and future direction. Cerebellum. 2013;12(2):245–66.
3. Jung BC, Choi SI, Du AX, Cuzzocreo JL, Geng ZZ, Ying HS, et al. Principal component analysis of cerebellar shape on MRI separates SCA type 2 and 6 into two archetypal modes of degeneration. Cerebellum. 2012;11:887–95.
4. Dohlinger S, Hauser TK, Borkert J, Luft AR, Schulz JB. Magnetic resonance imaging in spinocerebellar ataxias. Cerebellum [Res Support Non-US Gov't]. 2008;7(2):204–14.
5. Luft AR, Skalej M, Welte D, Kolb R, Burk K, Schulz JB, et al. A new semiautomated, three-dimensional technique allowing precise quantification of total and regional cerebellar volume using MRI. Magn Reson Med [Clin Trial]. 1998;40(1):143–51.
6. Good C, Johnsrude I, Ashburner J, Henson R, Friston K, Frackowiak R. A voxel-based morphometric study of aging in 465 normal adult human brains. Neuroimage. 2001;14:21–36.
7. Hadjivassiliou M, Currie S, Hoggard N. MR spectroscopy in paraneoplastic cerebellar degeneration. J Neuroradiol J Neuroradiol [Lett]. 2013;40(4):310–2.
8. Currie S, Hadjivassiliou M, Craven IJ, Wilkinson ID, Griffiths PD, Hoggard N. Magnetic resonance spectroscopy of the brain. Postgrad Med J. 2013;89(1048):94–106.
9. Braga-Neto P, Dutra LA, Pedroso JL, Felício AC, Alessi H, Santos-Galduroz RF, et al. Cognitive deficits in Machado-Joseph disease correlate with hypoperfusion of visual system areas. Cerebellum. 2012;11:1037–44.
10. Nanri K, Okita M, Takeguchi M, Taguchi T, Ishiko T, Saito H, et al. Intravenous immunoglobulin therapy for autoantibody-positive cerebellar ataxia. Intern Med. 2009;48:783–90.
11. Kimura N, Kumamoto T, Masuda T, Nomura Y, Hanaoka T, Hazama Y, et al. Evaluation of the effect of thyrotropin releasing hormone (TRH) on regional cerebral blood flow in spinocerebellar degeneration using 3DSRT. J Neurol Sci. 2009;281:93–8.
12. Kimura N, Kumamoto T, Masuda T, Nomura Y, Hanaoka T, Hazama Y, et al. Evaluation of the effects of thyrotropin releasing hormone (TRH) therapy on regional cerebral blood flow in the cerebellar variant of multiple system atrophy using 3DSRT. J Neuroimaging. 2011;21:132–7.
13. Lyoo CH, Jeong Y, Ryu YH, Lee SY, Song TJ, Lee JH, et al. Effects of disease duration on the clinical features and brain glucose metabolism in patients with mixed type multiple system atrophy. Brain. 2008;131:438–46.
14. Basu S, Alavi A. Role of FDG-PET in the clinical management of paraneoplastic neurological syndrome: detection of the underlying malignancy and the brain PET-MRI correlates. Mol Imaging Biol. 2008;10:131–7.
15. Wang PS, Liu RS, Yang BH, Soong BW. Topographic brain mapping of the international cooperative ataxia rating scale. A positron emission tomography study. J Neurol. 2007;254:722–8.
16. Inagaki A, Iida A, Matsubara M, Inagaki H. Positron emission tomography and magnetic resonance imaging in spinocerebellar ataxia type 2: a study of symptomatic and asymptomatic individuals. Eur J Neurol. 2005;12:725–8.
17. Soong B, Liu R. Positron emission tomography in asymptomatic gene carriers of Machado Joseph disease. J Neurol Neurosurg Psychiatry. 1998;64:499–504.
18. Brockmann K, Reimold M, Globas C, Hauser TK, Walter U, Machulla HJ, et al. PET and MRI reveal early evidence of neurodegeneration in Spinocerebellar Ataxia Type 17. J Nucl Med. 2012;53:1074–80.
19. Hosoi Y, Suzuki-Sakao M, Terada T, Konishi T, Ouchi Y, Miyajima H, et al. GABA-A receptor impairment in cerebellar ataxia with anti-glutamic acid decarboxylase antibodies. J Neurol. 2013. doi:10.1007/s00415-013-7092-y.
20. Varrone A, Salvatore E, De Michele G, Barone P, Sansone V, Pellecchia MT, et al. Reduced striatal [123I]FP-CIT binding in SCA2 patients without parkinsonism. Ann Neurol. 2004;55:426–30.
21. Kim JM, Lee JY, Kim HJ, Kim JS, Kim YK, Park SS, et al. The wide clinical spectrum and nigrostriatal dopaminergic damage in spinocerebellar ataxia type 6. J Neurol Neurosurg Psychiatry. 2010;81:529–32.
22. Kelp A, Koeppen AH, Petrasch-Parwez E, Calaminus C, Bauer C, Portal E, et al. A novel transgenic rat model for spinocerebellar ataxia type 17 recapitulates neuropathological changes and supplies in vivo imaging biomarkers. J Neurosci. 2013;33:9068–81.
23. Malinger G, Lev D, Lerman-Sagie T. The fetal cerebellum. Pitfalls in diagnosis and management. Prenat Diagn. 2009;29:372–80.
24. Limperopoulos C, Robertson Jr RL, Khwaja OS, et al. How accurately does current fetal imaging identify posterior fossa anomalies? Am J Roentgenol. 2008;190:1637–43.
25. Garel C. Posterior fossa malformations: main features and limits in prenatal diagnosis. Pediatr Radiol. 2010;40:1038–45.
26. Parazzini C, Righini A, Rustico M, Consonni D, Triulzi F. Prenatal magnetic resonance imaging: brain normal linear biometric values below 24 gestational weeks. Neuroradiology. 2008;50:877–83.
27. Hatab MR, Kamourieh SW, Twickler DM. MR volume of the fetal cerebellum in relation to growth. J Magn Reson Imaging. 2008;27:840–5.
28. Poretti A, Limperopoulos C, Roulet-Perez E, et al. Outcome of severe unilateral cerebellar hypoplasia. Dev Med Child Neurol. 2010;52:718–24.
29. Wong AM, Bilaniuk LT, Zimmerman RA, Liu PL. Prenatal MR imaging of Dandy-Walker complex: midline sagittal area analysis. Eur J Radiol. 2012;81:26–30.
30. Tarui T, Limperopoulos C, Sullivan NR, Robertson Richard L, du Plessis AJ. Long-term developmental outcome of children with a fetal diagnosis of isolated inferior vermian hypoplasia. Arch Dis Child Fetal Neonatal. 2014;99:54–8.
31. Klockgether T, Skalej M, Wedekind D, Luft AR, Welte D, Schulz JB, et al. Autosomal dominant cerebellar ataxia type I. MRI-based

volumetry of posterior fossa structures and basal ganglia in spinocerebellar ataxia types 1, 2 and 3. Brain. 1998;121(Pt 9): 1687–93.
32. Schulz JB, Borkert J, Wolf S, Schmitz-Hubsch T, Rakowicz M, Mariotti C, et al. Visualization, quantification and correlation of brain atrophy with clinical symptoms in spinocerebellar ataxia types 1, 3 and 6. Neuroimage. 2010;49:158–68.
33. Jacobi H, Reetz K, du Montcel ST, Bauer P, Mariotti C, Nanetti L, et al. Biological and clinical characteristics of individuals at risk for spinocerebellar ataxia types 1, 2, 3, and 6 in the longitudinal RISCA study: analysis of baseline data. Lancet Neurol. 2013;12:650–8.
34. Burk K, Abele M, Fetter M, Dichgans J, Skalej M, Laccone F, et al. Autosomal dominant cerebellar ataxia type I clinical features and MRI in families with SCA1, SCA2 and SCA3. Brain. 1996;119(Pt 5):1497–505.
35. Reetz K, Costa AS, Mirzazade S, Lehmann A, Juzek A, Rakowicz M, et al. Genotype-specific patterns of atrophy progression are more sensitive than clinical decline in SCA1, SCA3 and SCA6. Brain. 2013;136:905–17.
36. Della Nave R, Ginestroni A, Tessa C, Salvatore E, De Grandis D, Plasmati R, et al. Brain white matter damage in SCA1 and SCA2. An in vivo study using voxel-based morphometry, histogram analysis of mean diffusivity and tract-based spatial statistics. Neuroimage. 2008;43:10–9.
37. Solodkin A, Peri E, Chen EE, Ben-Jacob E, Gomez CM. Loss of intrinsic organization of cerebellar networks in spinocerebellar ataxia type 1: correlates with disease severity and duration. Cerebellum. 2011;10:218–32.
38. D'Agata F, Caroppo P, Boghi A, Coriasco M, Caglio M, Baudino B, et al. Linking coordinative and executive dysfunctions to atrophy in spinocerebellar ataxia 2 patients. Brain Struct Funct. 2011;216:275–88.
39. Schols L, Kruger R, Amoiridis G, Przuntek H, Epplen JT, Riess O. Spinocerebellar ataxia type 6: genotype and phenotype in German kindreds. J Neurol Neurosurg Psychiatry. 1998;64:67–73.
40. Lukas C, Schols L, Bellenberg B, Rub U, Przuntek H, Schmid G, et al. Dissociation of grey and white matter reduction in spinocerebellar ataxia type 3 and 6: a voxel-based morphometry study. Neurosci Lett. 2006;408:230–5.
41. Alcauter S, Barrios FA, Diaz R, Fernandez-Ruiz J. Gray and white matter alterations in spinocerebellar ataxia type 7: an in vivo DTI and VBM study. Neuroimage. 2011;55:1–7.
42. Rolfs A, Koeppen AH, Bauer I, Bauer P, Buhlmann S, Topka H, et al. Clinical features and neuropathology of autosomal dominant spinocerebellar ataxia (SCA17). Ann Neurol. 2003;54:367–75.
43. Lasek K, Lencer R, Gaser C, Hagenah J, Walter U, Wolters A, et al. Morphological basis for the spectrum of clinical deficits in spinocerebellar ataxia 17 (SCA17). Brain. 2006;129:2341–52.
44. Reetz K, Kleiman A, Klein C, Lencer R, Zuehlke C, Brockmann K, et al. CAG repeats determine brain atrophy in spinocerebellar ataxia 17: a VBM study. PLoS One. 2011;6:e15125.
45. Reetz K, Lencer R, Hagenah JM, Gaser C, Tadic V, Walter U, et al. Structural changes associated with progression of motor deficits in spinocerebellar ataxia 17. Cerebellum. 2010;9:210–7.
46. Reetz K, Dogan I, Rolfs A, Binkofski F, Schulz JB, Laird AR, et al. Investigating function and connectivity of morphometric findings—exemplified on cerebellar atrophy in spinocerebellar ataxia 17 (SCA17). Neuroimage. 2012;62:1354–66.
47. Hadjivassiliou M, Grünewald RA, Chattopadhyay AK, Davies-Jones GA, Gibson A, Jarratt JA, et al. Clinical, radiological, neurophysiological, and neuropathological characteristics of gluten ataxia. Lancet. 1998;352(9140):1582–5.
48. Wilkinson ID, Hadjivassiliou M, Dickson JM, Wallis L, Grünewald RA, Coley SC, et al. Cerebellar abnormalities on proton MR spectroscopy in gluten ataxia. J Neurol Neurosurg Psychiatry. 2005;76(7):1011–3.
49. Currie S, Hoggard N, Clark MJR, Sanders DS, Wilkinson ID, Griffiths PD, et al. Alcohol induces sensitization to gluten in genetically susceptible individuals: a case control study. PLoS One. 2013;8(10):e77638. doi:10.1371/journal.pone.0077638.
50. Currie S, Hadjivassiliou M, Clark MJ, Sanders DS, Wilkinson ID, Griffiths PD, et al. Should we be 'nervous' about coeliac disease? Brain abnormalities in patients with coeliac disease referred for neurological opinion. J Neurol Neurosurg Psychiatry. 2012;83(12):1216–21. doi:10.1136/jnnp-2012-303281.
51. Honnorat J, Saiz A, Giometto B, Vincent A, Brieva L, de Andres C, et al. Cerebellar ataxia with anti-glutamic acid decarboxylase antibodies: study of 14 patients. Arch Neurol. 2001;58(2):225–30.
52. Nanri K, Niwa H, Mitoma H, Takei A, Ikeda J, Harada T, et al. Low-titer anti-GAD-antibody-positive cerebellar ataxia. Cerebellum. 2013;12(2):171–5. doi:10.1007/s12311-012-0411-5.
53. Scheid R, Voltz R, Briest S, et al. Clinical insights into paraneoplastic cerebellar degeneration. J Neurol Neurosurg Psychiatry. 2006;77:529–30.
54. De Andrés C, Esquivel A, de Villoria JG, et al. Unusual magnetic resonance imaging and cerebrospinal fluid findings in paraneoplastic cerebellar degeneration: a sequential study. J Neurol Neurosurg Psychiatry. 2006;77:562–3.
55. Choi K-D, Kim JS, Park S-H, et al. Cerebellar hypermetabolism in paraneoplastic cerebellar degeneration. J Neurol Neurosurg Psychiatry. 2006;77:525–8.
56. Clapp AJ, Hunt CH, Johnson GB, Peller PJ. Semiquantitative analysis of brain metabolism in patients with paraneoplastic neurologic syndromes. Clin Nucl Med. 2013;38(4):241–7.
57. Hadjivassiliou M, Alder SJ, Van Beek EJR, Hannay MB, Lorenz E, Rao DG, et al. PET scan in clinically suspected paraneoplastic neurological syndromes: a six year prospective study in a regional neuroscience unit. Acta Neurol Scand. 2009;119:186–93.
58. Hadjivassiliou M, Boscolo S, Tongiorgi E, Grunewald RA, Sharrack B, Sanders DS, et al. Cerebellar ataxia as a possible organ specific autoimmune disease. Mov Disord. 2008;23(10):1270–377.
59. Hadjivassiliou M. Primary autoimmune cerebellar ataxia (PACA). ACNR. 2010;9(6):8–11.
60. Sunaga Y, Hikima A, Ostuka T, Morikawa A. Acute cerebellar ataxia with abnormal MRI lesions after varicella vaccination. Pediatr Neurol. 1995;13(4):340.
61. De Bruecker Y, Claus F, Demaerel P, Ballaux F, Sciot R, Lagae L, et al. MRI findings in acute cerebellitis. Eur Radiol. 2004;14(8):1478.
62. Daaboul Y, Vern BA, Blend MJ. Brain SPECT imaging and treatment with IVIg in acute post-infectious cerebellar ataxia: case report. Neurol Res. 1998;20(1):85.
63. Nagamitsu S, Matsuishi T, Ishibashi M, Yamashita Y, Nishimi T, Ichikawa K, et al. Decreased cerebellar blood flow in postinfectious acute cerebellar ataxia. J Neurol Neurosurg Psychiatry. 1999;67(1): 109.
64. Rapoport M, Reekum R, Mayberg H. The role of the cerebellum in cognition and behavior: a selective review. J Neuropsychiatry Clin Neurosci. 2000;12(2):193–8.
65. Baldaçara L, Borgio JGF, Moraes WAS, Lacerda ALT, Montaño MBMM, Tufik S, et al. Cerebellar volume in patients with dementia. Rev Bras Psiquiatr. 2011;33(2):122–9.
66. Schutter DJG, Honk J. The cerebellum in emotion regulation: a repetitive transcranial magnetic stimulation study. Cerebellum. 2009;8:28–34.
67. Miller TD, Ferguson KJ, Reid LM, Wardlaw JM, Starr JM, Seckl JR, et al. Cerebellar vermis size and cognitive ability in community-dwelling elderly men. Cerebellum. 2013;12:68–73.
68. Cabeza R, Nyberg L. Imaging cognition II: an empirical review of 275 PET and fMRI studies. J Cogn Neurosci. 2000;12:1–47.

69. Ramnani N. The primate cortico-cerebellar system: anatomy and function. Nat Rev Neurosci. 2006;7(7):511–22.
70. Hokkanen LSK, Kauranen V, Roine RO, Salonen O, Kotila M. Subtle cognitive deficits after cerebellar infarcts. Eur J Neurol. 2006;13(2):161–70.
71. Ravizza SM, McCornick CA, Schlerf JE, Justus T, Ivry RB, Fiez JA. Cerebellar damage produces selective deficits in verbal working memory. Brain. 2006;129:306–20.
72. Tadesco AM, Chiricozzi FR, Clausi S, Lupo M, Molinari M, Leggio MG. The cerebellar cognitive profile. Brain. 2011;134(Pt 12):3672–86.
73. Woodruff-Park DS, Vogel RW, Ewers M, Coffey J, Boyko OB, Lemieux SK. MRI-assessed volume of cerebellum correlates with associative learning. Neurobiol Learn Mem. 2001;76(3):342–57.
74. Luft AR, Skalej M, Schulz JB, Welte D, Kolb R, Burk K, et al. Patterns of age-related shrinkage in cerebellum and brainstem observed in vivo using three-dimensional MRI volumetry. Cereb Cortex. 1999;9(7):712–21.
75. Wegiel J, Wisniewski HM, Dziewiatkowski J, Badmajew E, Tarnawski M, Reisberg B, et al. Cerebellar atrophy in Alzheimer's disease—clinicopathological correlations. Brain Res. 1999;818(1):41–50.
76. Sjobeck M, Englund E. Alzheimer's disease and the cerebellum: a morphologic study on neuronal and glial changes. Dement Geriatr Cogn Disord. 2001;12(3):211–8.
77. Thomann PA, Schlafer C, Seidl U, Santos VD, Essig M, Schroder J. The cerebellum in mild cognitive impairment and Alzheimer's disease—a structural MRI study. J Psychiatr Res. 2008;42(14):1198–202.
78. Rombouts SA, van Swieten JC, Pijnenburg YA, Goekoop R, Barkhof F, Scheltens P. Loss of frontal fMRI activation in early frontotemporal dementia compared to early AD. Neurology. 2003;60(12):1904–8.
79. Yoon CW, Seo SW, Park J, Kwak KC, Yoon U, Suh MK, et al. Cerebellar atrophy in patients with subcortical-type vascular cognitive impairment. Cerebellum. 2013;12:35–42.
80. Whitwell JL, Weigand SD, Boeve BF, Senjem ML, Gunter JL, DeJesus-Hernandez M, et al. Neuroimaging signatures of frontotemporal dementia genetics: C9ORF72, tau, progranulin and sporadics. Brain. 2012;135(Pt 3):794–806.
81. Wu T, Hallett M. The cerebellum in Parkinson's disease. Brain. 2013;136(Pt 3):696–709.
82. Scharmüller W, Ille R, Schienle A. Cerebellar contribution to anger recognition deficits in Huntington's disease. Cerebellum. 2013;12(6):819–25.
83. Andersen K, Andersen BB, Pakkenberg B. Stereological quantification of the cerebellum in patients with Alzheimer's disease. Neurobiol Aging. 2012;33(1):197.e111–120.
84. Canu E, McLaren DG, Fitzgerald ME, Bendlin BB, Zoccatelli G, Alessandrini F, et al. Microstructural diffusion changes are independent of macrostructural volume loss in moderate to severe Alzheimer's disease. J Alzheimers Dis. 2010;19(3):963–76.
85. Moller C, Vrenken H, Jiskoot L, Versteeg A, Barkhof F, Scheltens P, et al. Different patterns of gray matter atrophy in early- and late-onset Alzheimer's disease. Neurobiol Aging. 2013;34(8):2014–22.
86. Bas O, Acer N, Mas N, Karabekir HS, Kusbeci OY, Sahin B. Stereological evaluation of the volume and volume fraction of intracranial structures in magnetic resonance images of patients with Alzheimer's disease. Ann Anat Anat Anz Off Organ Anat Ges. 2009;191(2):186–95.
87. Ishii K, Sasaki M, Kitagaki H, Yamaji S, Sakamoto S, Matsuda K, et al. Reduction of cerebellar glucose metabolism in advanced Alzheimer's disease. J Nucl Med. 1997;38(6):925–8.
88. Vidoni ED, Thomas GP, Honea RA, Loskutova N, Burns JM. Evidence of altered corticomotor system connectivity in early-stage Alzheimer's disease. J Neurol Phys Ther JNPT. 2012;36(1):8–16.
89. Nocuń A, Wojcza J, Szczepańska-Szerej H, Wilczyński M, Chrapko B. Quantitative evaluation of crossed cerebellar diaschisis, using voxel-based analysis of Tc-99m ECD brain SPECT. Nucl Med Rev Cent East Eur. 2013;16(1):31–4.
90. Sui R, Zhang L. Cerebellar dysfunction may play an important role in vascular dementia. Med Hypotheses. 2012;78(1):162–5. doi:10.1016/j.mehy.2011.10.017.
91. Jacova C, Hsiung GY, Tawankanjanachot I, Dinelle K, McCormick S, Gonzalez M, et al. Anterior brain glucose hypometabolism predates dementia in progranulin mutation carriers. Neurology. 2013;81(15):1322–31.
92. Asokan AG, D'souza S, Jeganathan Pai S. Fahr's syndrome—an interesting case presentation. J Clin Diagn Res. 2013;7(3):532–3.
93. Calabrò RS, Spadaro L, Marra A, Bramanti P. Fahr's disease presenting with dementia at onset: a case report and literature review. Behav Neurol. 2014;Article ID 750975, 3 pages. doi:10.1155/2014/75097.
94. Cohen OS, Hoffman C, Lee H, Champman J, Fulbright RK, Prohovnik I. MRI detection of the cerebellar syndrome in Creutzfeldt-Jackob Disease. Cerebellum. 2009;8:373–81.
95. Young GS, Geschwind MD, Fischbein NJ, Martindale JL, Henry RG, Liu S. Diffusion weighted and fluid-attenuated inversion recovery imaging in Creutzfeldt-Jakob disease: high sensitivity and specificity for diagnosis. AJNR Am J Neuroradiol. 2005;26:1551–62.
96. Ferrer I, Puig B, Blanco R, Martí E. Prion protein deposition and abnormal synaptic protein expression in the cerebellum in Creutzfeldt-Jakob disease. Neuroscience. 2000;97(4):715–26.
97. Brown P, Kenney K, Little B, Ironside J, Will R, Cervenáková L. Intracerebral distribution of infectious amyloid protein in spongiform encephalopathy. Ann Neurol. 1995;38:245–53.
98. Tanaka S, Saito M, Morimatsu M, Ohama E. Immunohistochemical studies of the PrP(CJD) deposition in Creutzfeldt-Jakob disease. Neuropathology. 2000;20:124–33.
99. Cooper SA, Murray KL, Heath CA, Will RG, Knight RS. Sporadic Creutzfeldt-Jakob disease with cerebellar ataxia at onset in the UK. J Neurol Neurosurg Psychiatry. 2006;77:1273–5.
100. Ortega-Cuberoa S, Luquína MR, Domínguezb I, Arbizub I, Pagolaa J, Carmona-Abellána MM, et al. Structural and functional neuroimaging in human prion diseases. Neurologia. 2013;28:299–308.
101. Ramos LR, Simoes EJ, Albert MS. Dependence in activities of daily living and cognitive impairment strongly predicted mortality in older urban residents in Brazil: a 2-year follow-up. J Am Geriatr Soc. 2001;49(9):1168–75.
102. Fatemi SH, Aldinger KA, Ashwood P, Bauman ML, Blaha CD, Blatt GJ, et al. Consensus paper: pathological role of the cerebellum in autism. Cerebellum. 2012;11(3):777–807.
103. Stoodley CJ, Schmahmann JD. Evidence for topographic organization in the cerebellum of motor control versus cognitive and affective processing. Cortex. 2010;46:831–44.
104. Skefos J, Cummings C, Enzer K, Holiday J, Weed K, Levy E, et al. Regional alterations in Purkinje cell density in patients with autism. PLoS One. 2014;9:e81255.
105. Fatemi SH, Stary JM, Halt AR, Realmuto GR. Dysregulation of Reelin and Bcl-2 proteins in autistic cerebellum. J Autism Dev Disord. 2001;31:529–35.
106. Gharani N, Benayed R, Mancuso V, Brzustowicz LM, Millonig JH. Association of the homeobox transcription factor, ENGRAILED 2, 3, with autism spectrum disorder. Mol Psychiatry. 2004;9(5):474–84.
107. Kuemerle B, Gulden F, Cherosky N, Williams E, Herrup K. The mouse *Engrailed* genes: a window into autism. Behav Brain Res. 2007;176(1):121–32.

108. Cheh MA, Millonig JH, Roselli LM, Ming X, Jacobsen E, Kamdar S, et al. *En2* knockout mice display neurobehavioral and neurochemical alterations relevant to autism spectrum disorder. Brain Res. 2006;1116(1):166–76.
109. Ieraci A, Forni PE, Ponzetto C. Viable hypomorphic signaling mutant of the Met receptor reveals a role for hepatocyte growth factor in postnatal cerebellar development. Proc Natl Acad Sci. 2002;99(23):15200–5.
110. Sousa I, Clark TG, Toma C, Kobayashi K, Choma M, Holt R, et al. MET and autism susceptibility: family and case–control studies. Eur J Hum Genet. 2009;17(6):749–58.
111. Vargas DL, Nascimbene C, Krishnan C, Zimmerman AW, Pardo CA. Neuroglial activation and neuroinflammation in the brain of patients with autism. Ann Neurol. 2005;57(1):67–81.
112. Fatemi SH, Folsom TD, Reutiman TJ, Thuras PD. Expression of GABAB receptors is altered in brains of subjects with autism. Cerebellum. 2009;8(1):64–9.
113. Fatemi SH, Reutiman TJ, Folsom TD, Huang H, Oishi K, Mori S, et al. Maternal infection leads to abnormal gene regulation and brain atrophy in mouse offspring: implications for genesis of neurodevelopmental disorders. Schizophr Res. 2008;99(1):56–70.
114. Courchesne E, Webb SJ, Schumann CM. From toddlers to adults: the changing landscape of the brain in autism. In: Amaral D, Geschwind D, Dawson G, editors. Autism spectrum disorders. Oxford: Oxford University Press; 2011. p. 611–31.
115. Stanfield AC, McIntosh AM, Spencer MD, Philip R, Gaur S, Lawrie SM. Towards a neuroanatomy of autism: a systematic review and meta-analysis of structural magnetic resonance imaging studies. Eur Psychiatry. 2008;23(4):289–99.
116. Verly M, Verhoeven J, Zink I, Mantini D, Peeters R, Deprez S, et al. Altered functional connectivity of the language network in ASD: role of classical language areas and cerebellum. NeuroImage Clin. 2014;4:374–82.
117. Catani M, Jones DK, Daly E, Embiricos N, Deeley Q, Pugliese L, et al. Altered cerebellar feedback projections in Asperger syndrome. Neuroimage. 2008;41(4):1184–91.
118. Cleavinger HB, Bigler ED, Johnson JL, Lu J, McMahon W, Lainhart JE. Quantitative magnetic resonance image analysis of the cerebellum in macrocephalic and normocephalic children and adults with autism. J Int Neuropsychol Soc. 2008;14(03):401–13.
119. Pierce K, Courchesne E. Evidence for a cerebellar role in reduced exploration and stereotyped behavior in autism. Biol Psychiatry. 2001;49(8):655–64.
120. Cheung C, Chua SE, Cheung V, Khong PL, Tai KS, Wong TKW, et al. White matter fractional anisotrophy differences and correlates of diagnostic symptoms in autism. J Child Psychol Psychiatry. 2009;50(9):1102–12.
121. Kates WR, Burnette CP, Eliez S, Strunge LA, Kaplan D, Landa R, et al. Neuroanatomic variation in monozygotic twin pairs discordant for the narrow phenotype for autism. Am J Psychiatr. 2004;161(3):539–46.
122. Webb SJ, Sparks BF, Friedman SD, Shaw DW, Giedd J, Dawson G, et al. Cerebellar vermal volumes and behavioral correlates in children with autism spectrum disorder. Psychiatry Res Neuroimaging. 2009;172(1):61–7.
123. Wang P, Erickson CA, Ginsberg G, Rathmell B, Cerubini M, Zarevics P. Of STX209 (arbaclofen) on social and communicative function in ASD: results of an 8 week open label trial. San Diego: International Meeting for Autism Research; 2011.
124. Ji L, Chauhan A, Brown WT, Chauhan V. Increased activities of Na+/K+−ATPase and Ca2+/Mg2+−ATPase in the frontal cortex and cerebellum of autistic individuals. Life Sci. 2009;85:788–93.
125. Anheim M, Tranchant C, Koenig M. The autosomal recessive cerebellar ataxias. N Engl J Med. 2012;366:636–46.
126. Brancati F, Dallapiccola B, Valente EM. Joubert syndrome and related disorders. Orphanet J Rare Dis. 2010;5:20.
127. Poretti A, Huisman TA, Scheer I, Boltshauser E. Joubert syndrome and related disorders: spectrum of neuroimaging findings in 75 patients. AJNR Am J Neuroradiol. 2011;32:1459–63.
128. Wallis LI et al. Proton spectroscopy and imaging at 3 T in ataxia-telangiectasia. AJNR Am J Neuroradiol. 2007;28:79–83.
129. Prodi E, Grisoli M, Panzeri M, Minati LF, Fattori F, Erbetta A, et al. Supratentorial and pontine MRI abnormalities characterize recessive spastic ataxia of Charlevoix-Saguenay. A comprehensive study of an Italian series. Eur J Neurol. 2013;20:138–46.
130. Rafiq M, Sharrack N, Shaw PI, Hadjivassiliou M. A neurological rarity not to be missed: cerebrotendinous xanthomatosis. Pract Neurol. 2011;11:296–300.
131. Della Nave R, Ginestroni A, Tessa C, Salvatore E, Bartolomei I, Salvi F, et al. Brain white matter tracts degeneration in Friedreich ataxia. An in vivo MRI study using tract-based spatial statistics and voxel based morphometry. Neuroimage. 2008;40:19–25.
132. Pagani E, Ginestroni A, Della Nave R, Agosta F, Salvi F, De Michele G, et al. Assessment of brain white matter fibre bundle atrophy in patients with Friedreich's ataxia. Radiology. 2010;255:882–9.
133. Akhlaghi H, Corben L, Georgiou-Karistianis N, Bradshaw J, Storey E, Delatycki MB, et al. Superior cerebellar peduncle atrophy in Friedreich's ataxia correlates with disease symptoms. Cerebellum. 2011;10:81–7.
134. Akhlaghi H, Yu J, Corben L, Georgiou-Karistianis N, Bradshaw JL, Storey E, et al. Cognitive deficits in Friedreich ataxia correlate with micro-structural changes in dentatorubral tract. Cerebellum. 2014;13:187–98.
135. Corben LA, Kashuk SR, Akhlaghi H, Jamadar S, Delatycki MB, Fielding J, et al. Myelin paucity of the superior cerebellar peduncle in individuals with Friedreich ataxia: an MRI magnetization transfer imaging study. J Neurol Sci. 2014. doi:10.1016/j.jns.2014.05.057.
136. Gilman S, Junck L, Markel DS, Koeppe RA, Kluin KJ. Cerebral glucose hypermetabolism in Friedreich's ataxia detected with positron emission tomography. Ann Neurol. 1990;28:750–7.
137. Iltis I, Hutter D, Bushara KO, Clark B, Gross M, Eberly LE, et al. ^{1}H MR spectroscopy in Friedreich's ataxia and ataxia with oculomotor apraxia type 2. Brain Res. 2010;1358:200–10.
138. De Stefano N, Dotti MT, Mortilla M, Federico A. Magnetic resonance imaging and spectroscopic changes in brain of patients with cerebrotendineous xanthomatosis. Brain. 2001;124:121–31.
139. Walterfang M, Fahey M, Abel L, Fietz M, Wood A, Bowman E, et al. Size and shape of the corpus callosum in adult Niemann–Pick type C reflects state and trait illness variables. AJNR Am J Neuroradiol. 2011;32:1340–6.
140. Walterfang M, Abel LA, Desmond P, Fahey MC, Bowman EA, Velakoulis D. Cerebellar volume correlates with saccadic gain and ataxia in adult Niemann-Pick type C. Mol Genet Metab. 2013;108:85–9.
141. Tedeschi G, Bonavita S, Barton NW, Bertolino A, Frank JA, Patronas NJ, et al. Proton magnetic resonance spectroscopic imaging in the clinical evaluation of patients with Niemann-Pick type C disease. J Neurol Neurosurg Psychiatry. 1998;65:72–9.
142. Brunberg JA, Jacquemont S, Hagerman RJ, Berry-Kravis EM, Grigsby J, Leehey MA, et al. Fragile X premutation carriers: characteristic MR imaging findings of adult male patients with progressive cerebellar and cognitive dysfunction. AJNR Am J Neuroradiol. 2002;23:1757–66.
143. Apartis E, Blancher A, Meissner WG, Guyant-Maréchal L, Maltête D, De Broucker T, et al. FXTAS: new insights and the need for revised diagnostic criteria. Neurology. 2012;79:1898–907.
144. Ginestroni A, Guerrini L, Della Nave R, Tessa C, Cellini E, Dotti MT, et al. Morphometry and 1H- MR spectroscopy of the brainstem and cerebellum in three patients with fragile-X premutation. AJNR Am J Neuroradiol. 2007;28:486–8.

145. Hashimoto R, Javan AK, Tassone F, Hagerman RJ, Rivera SM. A voxel-based morphometry study of grey matter loss in fragile X-associated tremor/ataxia syndrome. Brain. 2011;134:863–78.
146. Scaglione C, Ginestroni A, Vella A, Dotti MT, Della Nave R, Rizzo G, et al. MRI and SPECT of midbrain and striatal degeneration in fragile X-associated tremor/ataxia syndrome. J Neurol. 2008;255:144–6.
147. Parker CC, Evans OB. Metabolic disorders causing childhood ataxia. Semin Pediatr Neurol. 2003;10(3):193–9.
148. Barkovitch AJ. An approach to MRI of metabolic disorders in children. Approche IRM des maladies métaboliques de l'enfant. J Neuroradiol (Paris). 2007;34:75–88.
149. Beitzke D, Simbrunner J, Riccabona M. MRI in paediatric hypoxic-ischemic disease, metabolic disorders and malformations—a review. Eur J Radiol. 2008;68:199–213.
150. Pouwels JW, Vanderver A, Bernard G, Wolf Ni, Dreha-Kulczewksi SF, Deoni SCL, et al. Hypomyelinating leukodsystrophies: translational research progress and prospects. Ann Neurol. 2014.
151. Bricout M, Grévent D, Lebre AS, Rio M, Desguerre I, De Lonlay P, et al. Brain imaging in mitochondrial respiratory chain deficiency: combination of brain MRI features as a useful tool for genotype/phenotype correlations. J Med Genet. 2014;51:429–35.
152. Eichler F, Itoh R, Barker P, Mori S, Garrett ES, van Zijl PC, et al. Proton MR spectroscopic and diffusion tensor brain MR imaging in X-linked adrenoleucodystrophy: initial experience. Radiology. 2002;225(1):245–52.
153. Bianchi MC, Sgandurra G, Tosetti M, Battini R, Cioni G. Brain magnetic resonance in the diagnostic of mitochondrial encephalopathies. Biosci Rep. 2007;27(1–3):69–85.
154. Boddaert N, Romano S, Funalot B, Rio M, Sarzi E, et al. 1H MRS spectroscopy evidence of cerebellar high lactate in mitochondrial respiratory chain deficiency. Mol Genet Metab. 2008;93(1):85–8.
155. Steenweg ME, Vanderver A, Blaser S, Bizzi A, de Koning TJ, et al. Magnetic resonance imaging pattern recognition in hypomyelinating disorders. Brain. 2010;133:2971–82.
156. Ciolli L, Krismer F, Nicoletti F, Wenning GK. An update on the cerebellar subtype of multiple system atrophy. Cerebellum. 2014; in press.
157. Gilman S, Wenning GK, Low PA, Brooks DJ, Mathias CJ, et al. Second consensus statement on the diagnosis of multiple system atrophy. Neurology. 2008;71:670–6.
158. D'Abreu A, Cendes F. Neuroimaging of ataxia. Curr Clin Neurol. 2013;44:227–45.
159. Minnerop M, Lûders E, Specht K, Schimke N, Thompson PM, Chou YY, et al. Callosal tissues loss in multiple system atrophy—a one year follow-up study. Mov Disord. 2010;25:2613–20.
160. Matsusue E, Fujii S, Kanasaki Y, Ohama E, Ogawa T. Cerebellar lesions in multiple system atrophy: postmortem MR imaging-pathologic correlations. AJNR Am J Neuroradiol. 2009;30:1725–30.
161. Matsusue E, Fujii S, Kanasaki Y, Sugihara S, Miyata H, Ohama E, et al. Putaminal lesion in multiple system atrophy: postmortem MR-pathological correlations. Neuroradiology. 2008;50:559–67.
162. Specht K, Minnerop M, Müller-Hübenthal J, Klockgether T. Voxel-based analysis of multiple-system atrophy of cerebellar type: complementary results by combining voxel-based morphometry and voxel-based relaxometry. Neuroimage. 2005;25:287–93.
163. Loh KB, Rahmat K, Lim S-Y, Ramli N. A hot cross bun sign from diffusion tensor imaging and tractography perspective. Neurol India. 2011;59:266–9.
164. Yang H, Wang X, Liao W, Zhou G, Li L, Ouyang L. Application of tensor diffusion imaging in multiple system atrophy: the involvement of pontine transverse and longitudinal fibers. Int J Neurosci. 2014; in press.
165. Boesch SM, Wolf C, Seppi K, Felber S, Wenning GK, Schocke M. Differentiation of SCA2 from MSA-C using proton magnetic resonance spectroscopic imaging. J Magn Reson Imaging. 2007;25:564–9.
166. Kimura N, Kumamoto T, Nomura T, Hazama Y, Okazaki T. Evaluation of regional cerebral blood flow in cerebellar variant of multiple system atrophy using FineSRT. Clin Neurol Neurosurg. 2009;111:829–34.
167. Mazere J, Meissner WG, Sibon I, Lamare F, Tison F, Allard M, et al. [(123)I]-IBVM SPRECT imaging of cholinergic systems in multiple systems atrophy: a specific alteration of the ponto-thalamic cholinergic pathways (Ch5-Ch6). NeuroImage Clin. 2013;3:212–7.
168. Schulz JB, Klockgether T, Petersen D, Jauch M, Müller-Schauenburg W, Spieker S, et al. Multiple system atrophy: Natural history, MRI morphology and dopamine receptor imaging with 123IBZM-SPECT. J Neurol Neurosurg Psychiat. 1994;57:1047–56.
169. Hauser T, Luft A, Skalej M, Nägele T, Kircher T, Leube D, et al. Visualization and quantification of disease progression in multiple system atrophy. Mov Dis. 2006;18:85–92.
170. Abele M, Bûrk K, Schölsl, Schwartz S, Besenthal I, Dichgans J, et al. The aetiology of sporadic adult-onset ataxia. Brain. 2002;15:961–8.
171. Burk K, Globas C, Wahl T, Bürhing U, Dietz K, Zuhlke C, et al. MRI-based volumetric differentiation of sporadic cerebellar ataxia. Brain. 2004;127:175–81.